

1                   **Controls on the Distribution of Volcanism and Intra-Basaltic**  
2                   **Sediments in the Cambo-Rosebank Region, West of Shetland**

3                   Jonathon Hardman<sup>1\*</sup>, Nick Schofield<sup>1</sup>, David Jolley<sup>1</sup>, Adrian Hartley<sup>1</sup>, Simon Holford<sup>2</sup>,

4   Douglas Watson<sup>1</sup>

5                   <sup>1</sup> *Department of Geology and Petroleum Geology, University of Aberdeen, King's College, Aberdeen AB24*  
6   *3UE, UK*

7                   <sup>2</sup>*Australian School of Petroleum, Santos Petroleum Engineering Building, University of Adelaide, SA 5005,*  
8   *Australia*

9   \*Corresponding author (e-mail: [Jonathon.hardman@abdn.ac.uk](mailto:Jonathon.hardman@abdn.ac.uk))

10  
11                   **Abstract:** The magma-rich North Atlantic Margin is one of the last frontier areas of  
12 hydrocarbon exploration within the United Kingdom Continental Shelf. In 2004, a major oil  
13 and gas discovery (Rosebank) was made within Palaeocene to Eocene age lavas in the Faroe-  
14 Shetland Basin. The Rosebank field consists of intra-basaltic terrestrial to marginal marine  
15 reservoir sequences, separated by basaltic lava flows and volcanoclastics. Despite the  
16 identification of a major intra-lava incised drainage system running parallel to the SW-NE  
17 trending Rosebank Field, the controls on the distribution of both the volcanics and intra-  
18 volcanic sediments was previously unclear, in part due to the difficulties that volcanic  
19 sequences pose to seismic acquisition, processing and interpretation. This has led to  
20 uncertainty in defining the wider intra-basaltic play. However, the examination of the recently  
21 acquired FSB2011/12 MultiClient GeoStreamer® Survey has facilitated increased definition of  
22 the geological units within and below the volcanic succession, and a reinterpretation of the  
23 Late Palaeocene to Early Eocene stratigraphy. Through integration of 3D seismic data and well  
24 analysis we present a regional overview of the volcanics and intra-basaltic sediments in the  
25 Rosebank region of the Faroe-Shetland Basin. We find that the structural setting of the  
26 Rosebank Field, in addition to lava flow morphology, strongly influences the distribution of  
27 the intra-basaltic play-fairway within the Palaeocene-Eocene Flett Formation. Restriction of  
28 fluvial siliciclastic sediments adjacent to the Corona Ridge extends the theorised Rosebank  
29 play fairway to the area southwest of the Rosebank Field. Our analysis indicates that  
30 understanding basin structure is integral to the success of intra-basaltic plays.

31  
32 Hydrocarbon exploration in the Faroe-Shetland Basin (FSB), located on the Atlantic Margin  
33 of the United Kingdom Continental Shelf (UKCS), has been ongoing for the last 40 years.

34 Initially, during the early exploration history of the basin it was hoped that the FSB would  
35 mimic the prospectivity of the neighbouring North Sea. However, it has not met with the  
36 same success, being both technically and geologically challenging in terms of hydrocarbon  
37 exploration and production, in part due to the presence of igneous rocks throughout much  
38 of the basin (Varming *et al.*, 2012).

39 Throughout much of the Late Palaeocene and Early Eocene, the Faroe-Shetland Basin  
40 was subject to the eruption of up to 6.6 km of flood basalts, which form part of the Palaeogene  
41 North Atlantic Igneous Province and cover over 50% of the north-western side of the basin  
42 (White *et al.*, 2003; Schofield & Jolley, 2013) (Fig. 1). Despite heightened drilling activity in the  
43 early 2000's, the area of the basin covered by volcanics remains relatively underexplored and  
44 a frontier area for exploration (Varming *et al.*, 2012). The discovery of the Rosebank Field in  
45 2004, situated on the feather edge of the flood basalts, opened up a new play type within the  
46 basin with ~56.1 to 55.2 Ma siliciclastic dominated reservoir successions that developed within  
47 the volcanic succession during periods of volcanic quiescence (Duncan *et al.*, 2009; Poppitt *et*  
48 *al.*, 2016). Whilst fluvial channels have been identified within the Rosebank reservoir equivalent  
49 successions (Schofield & Jolley, 2013) the detailed stratigraphy and the controls on the  
50 emplacement of volcanics and intra-volcanic sedimentary rocks remains poorly understood  
51 both locally and regionally. In particular, the origin and wider distribution of the 'clean' sand  
52 units that form the Rosebank and intra-basaltic play fairway remain enigmatic (Schofield &  
53 Jolley, 2013).

54 The PGS and TGS Geostreamer® broadband seismic data, acquired in 2011/2012,  
55 spans the featheredge of the basalt cover imaging the transition from the Upper Palaeocene  
56 to Lower Eocene volcanics and similar age sediments in the Faroe-Shetland Basin (Fig. 2).  
57 Additionally, it provides a hitherto unprecedented view of basement structure and sill  
58 geometries in an area where intra and sub-basalt seismic imaging has been particularly

59 challenging (Spitzer *et al.*, 2008). The aim of this paper is to detail the stratigraphy of the Late  
60 Palaeocene/Early Eocene volcanic succession in the Faroe-Shetland Basin and investigate the  
61 controls on the distribution of volcanic and intra-basaltic sediments, by providing insights into  
62 the underlying basement structure. We also highlight the potential areas for further  
63 exploration within the volcanic successions of the Faroe-Shetland Basin.

64

## 65 **Geological History**

66

### 67 ***Regional Structure***

68

69 The Faroe-Shetland Basin consists of a series of SW-NE trending rift basins and structural  
70 highs that formed during episodic Mesozoic rifting (Fig. 1) (Duindam & Hoorn, 1987). The  
71 basin is bounded to the north and south by the Erlend Platform and the Wyville Thomson  
72 Ridge, respectively (Dore *et al.*, 1999). The Faroe-Shetland Basin can be divided into several  
73 sub-basins, of which the Judd, Foinaven, Flett and Corona are referred to in this study (Fig. 1).  
74 The most widely used stratigraphical scheme in the Faroe-Shetland Basin is the T-sequence  
75 scheme and although this was defined within the Judd and Foinaven basins in the SW of the  
76 basin (Ebdon *et al.*, 1995) (Fig. 3), it is used here for consistency with previous studies  
77 (Schofield & Jolley, 2013; Schofield *et al.*, 2015). Additionally, the standard UK Offshore  
78 Operators Association (UKOAA) lithostratigraphic nomenclature is used to refer to  
79 formations or key horizons (Fig. 3).

80 The tectonic evolution of the Faroe-Shetland Basin encompasses a number of rifting  
81 and compressional events that span a time period of ~400 Ma, from the Devonian to the  
82 Cenozoic (Dean *et al.*, 1999; Dore *et al.*, 1999). Onshore, the Caledonian orogeny formed a  
83 NE-SW trending basement grain throughout Scotland (Dean *et al.*, 1999). This structural grain

84 is thought to extend offshore into the NE Atlantic Margin, influencing subsequent tectonic  
85 events within the Faroe-Shetland Basin (Kimbell *et al.*, 2005). The basement grain is thought  
86 to have a long-lasting effect on the structural fabric of the Faroe-Shetland Basin, through  
87 nucleation of possible transfer zones (deep-seated shear zones) (Ellis *et al.*, 2009) and  
88 localisation of faults along pre-existing structural weaknesses (Moy *et al.*, 2009; Dore *et al.*,  
89 1997b).

90 Importantly, much of the Cenozoic basin structure within the Faroe-Shetland Basin  
91 was initiated during the Cretaceous. For a period of ~70 Myrs from the early Cretaceous, the  
92 Faroe-Shetland Basin underwent repeated rifting events and, in the Flett sub-basin, a 1000-  
93 3000 m thick, post-rift Cretaceous succession was deposited (Dean 1999).

94

#### 95 ***Palaeocene depositional environment within the FSB***

96

97 In the FSB, the early Palaeocene is represented by deep marine conditions with a series of  
98 basin floor fans that transported sands towards the basin centre from the basin margins such  
99 as the Judd High (Lamers & Carmichael, 1999). These basin floor fans were followed by  
100 deposition of the Lamba Formation (sequence T36 - T38, ~58.4– 56.1 Ma), which represents  
101 a major northerly progradational event within the Judd and Foinaven Sub-basins, recording a  
102 change from basal slope conditions to a deltaic succession composed of mudstones and  
103 subordinate sandstones (Shaw-Champion *et al.*, 2008). During this time, the shelf edge was  
104 positioned along the northern edge of the Westray High (marked by the northern extent of  
105 the Lamba Fm. clinoforms in Fig. 4). The upper Lamba Formation, (sequence T38), contains a  
106 number of north to north-westerly prograding clinoforms ~500 m high (Shaw-Champion *et*  
107 *al.*, 2008), which likely formed at or close to sea level as the delta front prograded into deeper  
108 water (Smallwood, 2002).

109           During the Late Palaeocene (sequence T38/T40 boundary), the FSB was uplifted and  
110 an erosional surface developed truncating the Lamba and underlying formations in the Judd  
111 and Foinaven Sub-Basins. (Morse, 2013; Champion, 2008). Coincident with uplift, eruption of  
112 the Faroe Island Basalt Group (FIBG) commenced at the onset of sequence T40 (56.1 Ma)  
113 with a series of flood basalts emplaced within the basin up to sequence T45 (~55.2 Ma;  
114 Schofield & Jolley, 2013). Siliciclastic sediments deposited within the volcanic succession  
115 ('intra-basaltic sediments') during this time period are collectively grouped within sequences  
116 T40 to T45 and referred to as the 'Colsay Member' of the Flett Formation (Duncan & Hansen,  
117 2009).

118           The supra-volcanic succession, sequence T45, termed the Hildasay Sandstone Member  
119 (Knox *et al.*, 1997), is more widely distributed in comparison to sequence T40, in places  
120 covering the T38/T40 unconformity, although it pinches out towards the basin bounding highs  
121 such as the Rona Ridge and the Solan Bank High (Ebdon *et al.*, 1995). Sequence T45 lowstand  
122 tracts are restricted to the centre of the Corona and Flett sub-basins area and deposited in a  
123 bathyal setting with highstand and transgressive tracts on the shelf deposited in a shallow to  
124 marginal marine setting (Ebdon *et al.*, 1995).

125           By the deposition of the Balder Formation (sequence T50), emplacement of lavas in  
126 the Faroe-Shetland region had ceased. The Balder Tuff member, contained within the lower  
127 part of the formation has typically been used as an historical seismic marker within the North  
128 Sea and the Faroe-Shetland Basin. This widespread tuff horizon has been linked to the incipient  
129 Greenland-Faroes rift and the initiation of seafloor spreading in the North Atlantic (Jolley &  
130 Bell, 2002; Jolley & Widdowson, 2005; Watson *et al.*, 2017).

131

132

133   **Overview of the Cambo-Rosebank Region**

134

135 The area surrounding the Cambo High, North of the Westray Ridge within the Faroe-Shetland  
136 Basin, presents an opportunity to gain a better understanding of the interplay between  
137 volcanics and intra-volcanic sediments (Figure 4). At the centre of the study area are two  
138 major structural highs; the Westray and Cambo Highs. The Cambo High (which covers an  
139 area of ~60 km<sup>2</sup>), drilled during evaluation of the Cambo prospect in 2002 (204/10- 1), is  
140 granodioritic in composition. Similarly, the Westray High (which covers an area of ~70 km<sup>2</sup>),  
141 although smaller in size, is granitic in composition (well 205/15-2). Both highs are thought to  
142 be Caledonian age igneous plutons as demonstrated by onlapping Cretaceous claystones (e.g.  
143 at the base of well 204/14-2) (Watson et al. 2017).

144 Two ridges extend to the north and south of the Cambo and Westray High. The  
145 northern Corona Ridge strikes ~150 km across the Faroe-Shetland Basin in a SW-NE  
146 direction. In the south, the top of the ridge is capped by the Jurassic Kimmeridge Clay  
147 Formation overlying Upper Jurassic Rona Formation sandstones and Carboniferous Clair  
148 Group sandstones (wells 213/27-1 and 213/27-2). Further to the north, the ridge is capped  
149 by Triassic sandstones situated above Carboniferous to Devonian age sediments (213/23-1).  
150 The ridge is overlapped by Cretaceous to Palaeocene age sediments along its extent and is  
151 consequently interpreted as a Mesozoic age tilted fault block that developed during  
152 Cretaceous aged rifting.

153 Of key stratigraphic and exploration importance in this study, is the Rosebank Field,  
154 located towards the southern extent of the Corona Ridge ~ 30 km north east of the Cambo  
155 High. Exploration wells targeting the Rosebank Field drilled three anticlinal closures within  
156 Rosebank and Rosebank North (Poppitt et al, 2016). The southern ridge, deemed the  
157 Westray, strikes ~30 km NNE-SSW and is generally capped by Jurassic sediments suggesting  
158 a similar origin to that of the Corona Ridge (204/15-2).

159

## 160 **Data and Methods**

161

162 The main dataset used in this study is the FSB2011/12 MultiClient GeoStreamer® survey.  
163 Covering an area of 2662 km<sup>2</sup>, the survey was acquired over the northern Westray Ridge, the  
164 Cambo High and the southwestern Corona Ridge, spanning the transition between a  
165 siliciclastic dominated terrain to the South to a volcanic terrain in the North (Fig. 3 & Fig. 4).  
166 Typically, conventional streamers suffer from near surface noise created by ocean waves.  
167 These creates ghosts that interfere at particular frequencies, dependent on streamer depth,  
168 attenuating certain parts of the frequency range (Fig. 5B). The Geostreamer® is a dual sensor  
169 marine streamer comprising of co-located hydrophones and vertical particle motion sensors  
170 that record both the upcoming and downgoing wavefield information (Fig. 5A). As the ghosts  
171 will be recorded with opposite polarity by the hydrophone and normal polarity by the particle  
172 motion sensors (Fig. 5B), the notches created by interference can be infilled by the  
173 complimentary spectra to create a deghosted frequency spectrum that records the full  
174 frequency bandwidth of the seismic data. Increased high frequencies reduce the dominant  
175 wavelength recorded within the seismic data and thus lead to finer vertical resolution of the  
176 seismic. Increased low frequencies help to reduce the side lobes contained within the data.  
177 Furthermore, the data used within this study had been processed a number of times by PGS  
178 prior to it being provided for interpretation. A dual sensor wave field separation was  
179 undergone to reduce the impact of mechanical noise on the particle motion sensor (Day *et*  
180 *al.*, 2013). A 3D surface-relation multiple elimination was used to suppress multiples within  
181 the data (e.g. Dandem & Verschuur, 1998). To further reduce the impact of multiples and  
182 noise on the seismic data, a high-resolution Radon demultiple was used (e.g. Hargreaves *et al.*,  
183 2001). Finally, an anisotropic Kirchhoff prestack time migration was used to improve imaging,

184 in particular for steeper events (Kirstiansen *et al.*, 2003). The interpretation conducted within  
185 this study was undertaken using the Final Kirchhoff PSTM Stack that has been waveshaped to  
186 zero phase. The data was not converted from time to depth.

187 The data is displayed with a reverse polarity, whereby a downward increase in acoustic  
188 impedance corresponds to a negative amplitude (red) reflection and a downward decrease in  
189 acoustic impedance is represented by a positive amplitude (blue) reflection. Basalt within the  
190 Rosebank Field has an interval velocity of  $\sim 3800 \text{ ms}^{-1}$  (taken from  $\sim 2987 \text{ m}$  measured depth  
191 in well 213/27- 2) with a dominant frequency of  $\sim 25 \text{ Hz}$  (taken from the Geostreamer<sup>®</sup> FSB  
192 2011/12 survey). These values were used to calculate a vertical resolution of  $\sim 38 \text{ m}$  for the  
193 extrusive volcanics in the Rosebank Field. Similarly, the intra-basaltic Colsay 3 of well 213/27-  
194 2 had an internal velocity of  $\sim 3000 \text{ m}$  (taken from  $\sim 2950 \text{ m}$ ) with a dominant frequency of  
195  $\sim 23 \text{ Hz}$  had a vertical resolution of  $\sim 32.5 \text{ m}$ .

196 Due to the preservation of both low and high frequencies in dual sensor streamers,  
197 the survey aides with better identification of geological units within and below the volcanic  
198 succession, especially at the lower frequencies required to image structures sub-basalt  
199 (Ziolkowski *et al.*, 2003). The broad nature of the frequency spectrum in broadband surveys  
200 is particularly useful for spectral decomposition, as more variation is observed in colour  
201 blends, aiding interpretation of horizons produced during seismic analysis (Szafian & Gómez-  
202 Martínez, 2015).

203 Within the confines of the FSB2011/2012 Geostreamer Survey, seventeen wells were  
204 used to aid analysis, ten of which drilled extrusive volcanics: Svinoy (6004/12 – 1); six wells  
205 from the Rosebank Field (205/01-1, 213/26-1, 213/27-1, 213/27-2, 213/27-3, 213/27-4) (Figs.  
206 5 & 6) and four wells from the Cambo Field, a nearby four-way closure consisting of Lower  
207 Eocene deltaic to shoreface sands (Fielding *et al.*, 2014) (204/10-1, 204/10-2, 204/10a-3,  
208 204/10a-4) (Fig. 5). A 1D synthetic seismic was generated from the southern Rosebank wells



209 within the Geostreamer<sup>®</sup> survey (205/01- 1 and 213/26- 1), using the sonic and density  
210 wireline data throughout the post-volcanic and volcanic succession (Fig. 6). Velocity data for  
211 all wells within the survey was of high quality (i.e. well headers matched with the seismic well  
212 tie) and the well tie facilitated correlation of the Rosebank wells with the Cambo wells (Fig.  
213 7).

## 214 **Distribution and Stratigraphy of Volcanics and Intra-volcanic Sediments**

215

216 Where penetrated by wells in the study area, the volcanic succession reaches thicknesses of  
217 up to ~ 120 m, thickening into the Flett and Corona Basins and thinning towards the Westray  
218 High in the south. The intra-basaltic units in the study area have been deemed the Colsay  
219 Member of the Flett Formation (Duncan & Hansen, 2009). The Colsay Member was further  
220 divided into numbered units based on their stratigraphic level in the sequence (Fig. 8). The  
221 first intra-volcanic sequence penetrated was deemed Colsay 1, the second Colsay 2 and so  
222 on. The volcanics in the region were not numbered, but given a broader name of Upper,  
223 Middle or Lower dependent on their relative level in the sequence (Fig. 8). Here, we provide  
224 a detailed description and interpretation of the different units within the volcanics succession,  
225 based on the seismic and well analysis conducted within this study. In order to capture the  
226 evolution of the study area, we start at the base of the succession (Colsay 4) and work up  
227 from there. A detailed description and interpretation of the different units within the volcanic  
228 succession is presented below.

229

### 230 **Colsay 4**

231

232 The base of the volcanic succession is marked by a regionally extensive seismic 'soft kick' that  
233 ties back to the Colsay 4 unit and similar-aged volcanoclastic sediments in the available wells

234 (Fig. 7). Deposition of Colsay 4 sediments precedes the eruption of the Rosebank Lower  
235 Volcanics and this stratigraphic marker onlaps the Cambo and Westray Highs. Typically  
236 volcanoclastic in lithology, Colsay 4 overlies marine shales at the base of the volcanic succession  
237 with the transition marked by a ~ 5 m thick coarsening upwards siltstone package overlying a  
238 thick, Lower Palaeocene claystone succession. In the south of the Rosebank Field,  
239 volcanoclastic sediments typically consist of interbedded claystones and siltstones and to the  
240 north they grade into alternating siltstone and volcanoclastic sandstone beds. Notably, in wells  
241 drilled off crest of the Corona ridge (213/26-1, 213/27-2), thin (~10 m) packages of siliciclastic  
242 sandstones were encountered at the very top of the Colsay 4 succession (Fig. 8).

243

#### 244 ***Interpretation***

245

246 Colsay 4 is a regressive package that developed prior to the eruption of volcanics in  
247 the study area. The absence of volcanics and the presence of volcanoclastic sediments in the  
248 Rosebank and Cambo Wells suggests that early T40 age eruptions were not drilled by available  
249 wells, but were being actively eroded. This conforms to palynological work that also suggests  
250 Cycle I and basal Cycle II volcanics present on the Faroe Islands are not present in the  
251 Rosebank region (Jolley *et al.* 2012).

252 Colsay 4 siliciclastic sediments were encountered at the very top of the sequence by wells  
253 drilled off-structure (213/26-1, 213/27-2), but were absent in wells drilled on top of the  
254 Corona ridge (e.g. 213/27- 1) (Fig. 8), This suggests that, prior to eruption of the Rosebank  
255 Lower Volcanics, the sides of structural highs, such as the Corona and Westray Ridges, were  
256 a focal point for transportation of siliciclastic sediments.

257

#### 258 ***Rosebank Lower Volcanics (RLV)***

259

260 Rosebank Lower Volcanics (RLV) cover much of the study area and are encountered by all  
261 Rosebank wells. Volcanics of this age are also encountered on the Cambo Structure. The  
262 Rosebank Lower Volcanics form a seismic 'hard-kick' that brightens north of the Corona  
263 Ridge, thinning onto palaeohighs and towards the south of the study area (6004/12-1z). The  
264 RLV can be confidently tied back to the 213/26-1 well where the contact between Colsay 3  
265 sediments and the Rosebank Lower Volcanics is clearly imaged (Fig. 6). Basal sequence T40  
266 flows are thin (~7 m) and characteristically tabular classic lava flows with thin basal crusts and  
267 thick upper crusts (Nelson *et al.*, 2009a; Millett *et al.*, 2016) (Fig. 8). These basal flows are  
268 most common on the northern side of the Corona ridge (213/26-1). The top of the RLV  
269 succession in the south of the Rosebank Field is typically marked by a ~40 to 50 m thick flow.  
270 The petrophysical characteristics of the Rosebank Lower Volcanics flows resemble those of  
271 compound lava flows, possessing a consistently high density (~2.55–2.7 g/cm<sup>3</sup>), and a  
272 consistently high sonic velocity (~45–80  $\mu$ s/ft) (Fig. 9) (Millett *et al.*, 2016). The whole  
273 succession thins considerably toward Rosebank North (213/27- 3) where only a couple of  
274 small lava flows are observed (~3 – 7 m). In the South of the study area, Svinoy (6004/12-1)  
275 penetrated a thin (5 m) T40 volcanic package, highlighting the widespread nature of T40 aged  
276 volcanics.

277

## 278 **Interpretation**

279

280 Located at the base of the volcanic succession, the sequence T40 volcanics are of equivalent  
281 age to the Upper Beinivørð Formation of the FIBG (Cycle 2 of Jolley *et al.* 2012). Well and  
282 seismic data suggest that, initially, classic tabular lava flows were emplaced over a regionally

283 extensive area. Subsequent sequence T40 volcanism is recorded by more localised compound  
284 lava flows (213/26-1).

285

### 286 **Colsay 3**

287

288 North of the Corona Ridge, the Colsay 3 seismic horizon is a high amplitude, laterally  
289 continuous positive seismic reflection (Fig. 7). Within the south of the Rosebank Field, the  
290 Colsay 3 package is relatively thin (~10 m thick) consisting mainly of floodplain (213/26-1) and  
291 fluvial (205/01-1) sedimentary packages (Fig. 10). The sequence thickens considerably into the  
292 central Rosebank wells, where thick (~50 m) successions of alternating sandstones, claystones  
293 and siltstones indicative of an estuarine environment are recorded (Schofield & Jolley, 2013).  
294 These successions were cored during the drilling of the 213/27-2 well where the sandstone  
295 composition is dominantly quartzose and feldspathic (Fig. 10). In Rosebank North, the  
296 sequence continues to thicken (~120 m), and is dominated by siltstone with a few influxes of  
297 volcanoclastic sandstone.

298         The Colsay 3 reflector was also mapped to the south of the Corona Ridge where it  
299 dims to the north of the T38/T40 unconformity. In RMS amplitude extraction and spectral  
300 decomposition of this horizon, a linear feature, with an axis orientated SW-NE, can be  
301 observed between the Cambo High and the southern extent of the Rosebank Field (Fig. 11).  
302 The Cambo High is a palaeohigh in the Cambo-Rosebank area that has a provenance of 400-  
303 500 m relative to the Corona Ridge. On the Cambo High, the linear feature is a ~5 km wide  
304 topographical low that thins towards the south of the Rosebank Field where it is intersected  
305 by the 205/01-1 well. A similar topographic low is observed to the north of the Corona  
306 Ridge, coinciding with the proposed intra-basaltic drainage system imaged by Schofield & Jolley  
307 (2013).

308

309 **Interpretation**

310

311 The Colsay 3 unit marks a hiatus in volcanism in the Faroe-Shetland Basin significant enough  
312 to allow a dominantly siliciclastic sedimentary environment to re-establish itself in the greater  
313 Rosebank and Cambo area. The fluvial to estuarine, non-volcaniclastic facies observed here,  
314 alongside the orientation of the SW-NE trending intra-basaltic fluvial system described by  
315 Schofield & Jolley (2013), suggest that Colsay 3 is largely sourced from the area south of the  
316 flood basalts, where sources of clean sediment exist. However, through core analysis and  
317 seismic geomorphology of the Colsay 3 reflector, we also recognise local contributors to  
318 intra-volcanic sedimentation. Due to its seismic character and the dominance of fluvial  
319 sedimentary facies in well 205/01-1 (Poppitt *et al.*, 2016), the linear feature running between  
320 the Cambo and Rosebank Field, is interpreted as a topographic low exploited by a fluvial  
321 system. Due to the concurrent deposition of coarse grains of quartz and feldspar within  
322 Colsay 3 (e.g. 213/27-2 Colsay 3 cored sequence, Fig. 10) and what appears to be subaerial  
323 exposure of parts of the granodioritic Cambo High during deposition of Colsay 3 (Fig. 11), we  
324 suggest that parts of the Colsay 3 succession in Rosebank are sourced relatively locally from  
325 the Cambo High (20 km away).

326

327 **Colsay 2**

328

329 The Colsay 2 volcanic and intra-volcanic unit is a laterally extensive negative seismic reflection  
330 that brightens significantly on the northern edge of the Corona Ridge (Fig. 6 & 7). Similarly, it  
331 is penetrated by all Rosebank wells in the study area (Fig. 8). Where penetrated, top Colsay  
332 2 is marked by a basalt flow that thins (from ~20 m to 0 m) towards Rosebank North where

333 it grades to volcanoclastic sandstones. In the centre of the Rosebank Field (wells 213/27-1, 2  
334 and 4) there is a thin (~10 m) siliciclastic Colsay 2 intra-basaltic package that thickens towards  
335 Rosebank North (~ 40 m) (Fig. 8). To the south (as cored by 205/01-1), the top of the Colsay  
336 2 intra-basaltic package is marked by volcanoclastic siltstones, siltstones and lignitic material.  
337 Whilst north of the Corona Ridge the Colsay 2 reflector is a laterally extensive negative  
338 seismic reflection, progressively south of the Corona Ridge, the reflection appears less bright,  
339 thinner, and more fragmented (Fig. 7). It is seen to onlap the T38/T40 unconformity on the  
340 northern side of the Westray High. In well 205/01-1, relative to well 213/26-1, the intersection  
341 of the linear feature between Cambo and Rosebank (imaged in the Colsay 3 spectral  
342 decomposition) corresponds with an increase in the proportion of volcanoclastic sandstones  
343 (Fig. 7).

344

### 345 ***Interpretation***

346

347 The Colsay 2 member records a period of lower volcanic activity in the Rosebank-Cambo  
348 region, during which siliclastic sedimentary systems compete with the volcanics for  
349 accommodation space. Many of the features identified in Colsay 3, such as the potential  
350 drainage systems parallel to the Corona Ridge, remain established during this period of time.  
351 As siliciclastic systems remain active alongside the volcanics during Colsay 2, it is likely that  
352 any drainage systems contain a large proportion of volcanoclastic and siliciclastic material  
353 relative to the surrounding area (e.g. well 205/01-1 and the topographic lows in Figure 9). The  
354 basalt flows intersected by well 213/26-1, are potentially a source for volcanoclastic sandstones  
355 in the Rosebank Field.

356

### 357 ***Colsay 1***

358

359 Within the FSB 2011/2012 Survey, the Colsay 1 reflector is the most laterally extensive,  
360 prominent positive seismic reflection within the volcanic succession (Fig. 6 & Fig. 7). North of  
361 the Cambo High, the reflector is continuous, brightening north of the Corona Ridge. The  
362 bright area abuts the Corona Ridge and this increase in brightness is marked by a shift to  
363 higher frequencies observed through use of spectral decomposition (Fig. 11). South of the  
364 Cambo High, the reflector becomes much less continuous and less bright until it onlaps the  
365 T38/T40 unconformity in the region of the Westray High (~ 5 km north of well 204/14-2, Fig.  
366 4).

367 The Colsay 1 member can be confidently tied back to all available Rosebank Wells  
368 (Fig. 6, 7 & 8) although it is not intersected by any of the Cambo wells available. Notably, the  
369 base of the unit is marked by a ~5 m fining upwards package and an influx of siltstone. The  
370 Colsay 1 reflector nearly drapes the Cambo High, suggesting that it was nearly buried during  
371 Colsay 1 times (Fig. 7). Notably, the linear feature running between Cambo and the Corona  
372 Ridge, visible within the Colsay 2 and 3 units is fainter when imaged on the Colsay 1 reflection  
373 (Fig. 11).

374

### 375 ***Interpretation***

376

377 The Colsay 1 intra-volcanic member records a significant hiatus in volcanic activity, several  
378 marine transgressions and the boundary between T40 and T45 in the study area. In the central  
379 Rosebank wells, the basal section of Colsay 1 is sequence T40. Sediments of this age are  
380 typically fluvial sandstones, similar in composition to Colsay 3. Sequence T40 Colsay  
381 sediments are capped by a major transgression marked by an influx of shales and siltstones,  
382 and the overlying Colsay 1 package is sequence T45 in age and fully marine. An increase in the

383 brightness of the Colsay 1 reflector to the north of the Corona Ridge (observable in Fig. 7A)  
384 is marked by an increase in the abundance of siltstones and claystones relative to sandstones  
385 in Colsay 1, from 47% of the succession (205/01-1) to 62% (213/26-1). This change in seismic  
386 and sedimentary facies just north of the Corona Ridge, is taken to be an approximate position  
387 of the coastline during Colsay 1.

388         The lack of a feature corresponding to the proposed drainage system imaged between  
389 Cambo and Rosebank in Colsay 3 suggests that, by the end of Colsay 1, the drainage system  
390 had become infilled by a combination of late stage T40 volcanics and the Colsay 2 and 3  
391 successions in the area.

392

393

#### 394 **Rosebank Upper Volcanics**

395

396 The Rosebank Upper Volcanics, situated towards the top of the volcanic succession, are some  
397 of the most clearly imaged lava flows observed within the seismic data (Fig. 13). Seismically,  
398 the Upper Volcanics form a negative seismic reflection representative of the transition  
399 between the overlying volcanoclastics and the lava flows themselves. The lava flows have a  
400 particularly discontinuous seismic response and individual flow lobes can be identified (Fig.  
401 13B). Their petrophysical character differs from the lower volcanics in displaying a saw tooth  
402 texture density and sonic, typical of compound lava flows (Millett *et al.*, 2016) (see Fig. 9). In  
403 RMS amplitude extractions of the horizons, the lava flows form relative bright spots.

404         Unlike the underlying successions, the lateral extent of the Rosebank Upper Volcanics  
405 is constrained to the area surrounding the Corona Ridge, with the full extent of the horizon  
406 mapped shown by Figure 13. A major vent structure (1 x 1.5 km) situated ~1 km south of the  
407 205/01-1 well was clearly imaged with separate lava flows flowing either north into troughs in



408 the Corona Ridge, or South into the Flett Basin (Schofield *et al.*, 2015). The vent structure is  
409 situated directly above the minimum depth reached by an underlying sill and disruption in the  
410 seismic beneath the vent structure may represent the plumbing system of this vent (Fig. 13).  
411 A similar feature is noted north of the Corona Ridge, where the presence of a smaller lava  
412 flow is coincident with a vent positioned above the flow lobe of a sill (Fig. 13).

413

#### 414 ***Interpretation***

415

416 The Rosebank Upper Volcanics are a series of lava flows representing the subaerial eruption  
417 of basalt following deposition of Colsay I. Compound lava flows of this age are stratigraphically  
418 equivalent to the Malinstindur Formation in the Faroe Islands Basalt Group (Passey & Jolley,  
419 2008). Despite this, the range of thicknesses observed in the available wells and the variability  
420 in the areal extent of the lava flows observed in the study area highlights that basinal eruptions  
421 were separate volcanic events from those on the Faroe Islands. The coincidence of the Faroe-  
422 Shetland Sill Complex with eruptive centres highlights the importance of sills in facilitating  
423 magma transport within the Faroe-Shetland Basin (Schofield *et al.*, 2015).

424

#### 425 ***Rosebank Upper Volcaniclastics***

426

427 The Rosebank Upper Volcaniclastics represent the uppermost section of the volcanic  
428 succession in the wider Rosebank and Cambo area. They are identified as a bright negative  
429 seismic reflection that is identifiable over the entire FSB2011/2012 survey (Fig. 7). In Rosebank,  
430 the Rosebank Upper Volcaniclastics are typically volcaniclastic (predominantly volcaniclastic  
431 sandstone) sedimentary rocks of sequence T45 in age. The unit differs in the Cambo region  
432 where the first volcanic units encountered are basalts interbedded with predominantly

433 volcanoclastic claystones (Fig. 8). Wells 213/27-2 and 213/27-4 of Rosebank are devoid of  
434 volcanoclastic sandstone and are wholly made up of volcanoclastic claystones and siltstones  
435 (Fig. 14).

436

### 437 ***Interpretation***

438

439 Rosebank Upper Volcaniclastics appear to be the weathering products of underlying and  
440 nearby lava flows. As coarser grained epiclastic volcanoclastics are generally deposited more  
441 proximal to eroded parent bodies (Fisher, 1961), coarse-grained volcanoclastics in the south  
442 of the Rosebank Field are correlated with the sequence T45 eruptive centre proximal to the  
443 south of the Rosebank Field (Fig. 13). Lava flows on the Cambo High remained exposed  
444 throughout much of the deposition of the Upper Volcaniclastics and were potentially a source  
445 for volcanoclastics seen in well 204/10a-3 (Cambo) and 205/01-1.

446

### 447 ***Upper Sequence T45 Lava Flows (Enni Equivalent)***

448

449 The upper lava flows are represented by a bright hard kick restricted to the north of the  
450 Cambo High and Corona Ridge. Although not penetrated by any wells, the horizon mapped  
451 extends towards the 213/26-1 and 205/01-1 wells in the south of the Rosebank Field where  
452 the sequence is dominated by volcanoclastic sandstones representing the erosive products of  
453 nearby basalt flows. Spectral decomposition was undertaken on the horizon mapped with lava  
454 flows appearing as a zone of high relative amplitude within the data (Fig. 15). The brightness  
455 of the upper lava flows attenuates and scatters the seismic signal, leading to ghosting in the  
456 underlying Rosebank Upper Volcaniclastics.

457

## 458 **Interpretation**

459

460 Onshore the Faroe Islands, the sequence T45 Enni Formation represents the youngest  
461 sequences in the FIBG. They are typically extensive compound lava flows with a MORB-like  
462 composition (Rasmussen & Noe-Nygaard 1970; Waagstein *et al.* 2002). The very uppermost  
463 flows identified in the study area are stratigraphically equivalent to the Enni Formation due to  
464 their stratigraphical position at the very top of the volcanic sequence (Schofield & Jolley, 2013).

465

## 466 **Isochron Thickness of the Colsay Sequences**

467

468 Isochron thickness maps were created for the most regionally extensive volcanic  
469 horizons and used as a proxy for the thickness of volcanics and intra-volcanic sediments.  
470 Figure 16 shows an isochron thickness map between base Colsay 1 and top Upper  
471 Volcaniclastics, encompassing Colsay 1 sediments, the Rosebank Upper Volcanics and the  
472 Rosebank Upper Volcaniclastics. Notably, two areas of thickening exist either side of the  
473 Corona Ridge. The northern area coincides with the proposed fluvial system identified by  
474 Schofield & Jolley (2013), whilst the southern area coincides with the Colsay 3 and Colsay 2  
475 proposed drainage system. As such, thickness maps provide evidence that areas either side  
476 of the Corona Ridge were prone to repeated exploitation by fluvial sedimentation. However,  
477 the Rosebank Upper Volcanics lava flows are also observed infilling the lows either side and  
478 within the Corona Ridge (Fig. 13A and D). Therefore, areas of thickened siliciclastic  
479 successions may also coincide with areas of thickened volcanics.

480

## 481 **Discussion**

482

## 483 **Palaeogeographic Evolution of the Cambo-Rosebank Region**

484

485 The interpretation of several seismic datasets combined with the petrophysical analysis and  
486 correlation of available wells allows the stratigraphic evolution of the Late Palaeocene to Early  
487 Eocene volcanic succession to be determined. Initial interpretations of the Rosebank Field  
488 envisaged the Corona Ridge as a palaeohigh that acted as a focal point for the interfingering  
489 of volcanics and siliciclastic sediments prograding from the North West and South East,  
490 respectively (Helland-Hansen 2009). However, on the basis of new data, the following  
491 palaeogeographic settings have been reconstructed for the Upper Palaeocene and Lower  
492 Eocene (Fig. 17). Notably, during periods of volcanic quiescence (Fig. 17A), siliciclastic  
493 sedimentary systems are able to build out into the centre of the Faroe-Shetland Basin towards  
494 highs such as the Corona Ridge. During periods of volcanic activity, these sedimentary systems  
495 are diverted away from areas of active eruption (Fig. 17B). The controls on the location of  
496 sedimentary systems and areas of active eruption are discussed.

497

## 498 **Controls on the Distribution of Colsay Member Sequences**

499

500 During the eruption and emplacement of continental flood basalts, pre-existing fluvial systems  
501 may be overwhelmed or diverted. During periods of volcanic quiescence, fluvial systems may  
502 become re-established if their catchments are located in areas that are not influenced by  
503 volcanism (Ebinghaus et al. 2014). The distribution and development of intra-basaltic drainage  
504 systems during periods of quiescence are strongly influenced by the topography created by  
505 preceding lava flows (Reidel et al., 2013) in addition to the pre-existing topographic lows that  
506 were not filled by lavas (Schofield & Jolley, 2013; Ebinghaus et al., 2014).

507           The predictable evolution of continental flood basalts has been recognised within Large  
508 Igneous Provinces (Jerram & Widdowson 2005). During the inception of a Large Igneous  
509 Province, low volumes of lava erupt directly onto pre-existing bedrock. During this stage, the  
510 pre-eruption topography exerts a control on distribution of eruptive products (Beeson *et al.*,  
511 1989). The main phase of a flood basalt province is marked by repeated eruption of a number  
512 of high volume lava flows that cover large areas (e.g. 6340 km<sup>2</sup> for the Springbok-PAV unit B  
513 in the Parana-Etendeka province; Jerram & Widdowson 2005), originating from a number of  
514 spatially restricted eruption sites and fissures. Whilst the location of the eruption sites and  
515 fissures is largely controlled by lithospheric and crustal weaknesses, the distribution of lava  
516 flows is also controlled by lava sheet topography and infilling of topography by other flows or  
517 intra-volcanic sediments. The overall duration of this main stage is typically in the order of  
518 500 kyr (Baksi, 1988; Jerram & Widdowson, 2005). During the final stage of volcanism, the  
519 eruption volumes decrease and eruption centres become more widely distributed.

520

521 Additionally, small scale changes in individual lava flows and sedimentary systems are imposed  
522 on the large scale changes described above.

- 523       • Channelized or intra-canyon lava flows are generated by flow into a pre-existing  
524       topographic low primarily controlled by tectonic activity and pre-existing erosional  
525       surface topography (Beeson *et al.*, 1989).
- 526       • Sheet like lava flows indicate low, relatively flat topographic relief. Drainage systems  
527       with source areas outside the lava field are likely to dam and buttress against the lava  
528       field, or flow around it (Beeson *et al.*, 1989).
- 529       • Deep and wide topographic lows such as river valleys are often preserved during lava  
530       flow-emplacment, promoting re-establishment of drainage systems along their  
531       pathway (Schofield and Jolley, 2013).

532

533 The Faroe-Shetland Basin is divided into a series of NE-SW trending sub-basins that have  
534 acted as depocentres from the Cretaceous to the present-day (Ritchie *et al.*, 2011). In the  
535 study area, basement highs such as Cambo and Westray are granodioritic to granitic in  
536 composition and thus more resistive to faulting and erosion (Watson *et al.* 2017). The  
537 basement ridges adjacent to the Cambo and Westray Highs (the Westray and Corona ridges)  
538 typically consist of Jurassic and older sediments that were downthrown deeper into the basin  
539 during Cretaceous rifting. In the Faroe-Shetland Basin, this structural heterogeneity strongly  
540 controls the distribution of Colsay Member sequences within the Rosebank Field. Parallel to  
541 the sides of the Corona Ridge, palaeolows were repeatedly exploited by volcanics and intra-  
542 basaltic sediments, illustrated by the isochron thickness map (Fig. 16) and fluvial sediments in  
543 205/01-1. The continual expression of these topographical lows throughout the emplacement  
544 of the volcanic succession suggests that topography generated prior to eruption of the T40  
545 lava flows was not infilled and bypassed by later volcanic or sedimentary events. Instead,  
546 longstanding topographical lows either side of the Corona Ridge were exploited repeatedly  
547 by volcanism and intra-basaltic units. It has been suggested that the lack of faulting throughout  
548 the Palaeocene of the Faroe-Shetland Basin is due to accommodation of extension in upper  
549 Cretaceous shales (Dean 1999). Notably, the greatest thicknesses of the tertiary sediment  
550 typically overly the thickest Cretaceous successions. Therefore, we might expect that the  
551 thickest Cretaceous successions, found within the lows of the Corona Ridge, differentially  
552 compact during deposition of the volcanic sequences generating the topographical lows  
553 observed here.

554

### 555 ***Controls on the Distribution of Volcanics***

556

557 In addition to lava flows and intra-basaltic sediments infilling ridge-adjacent topographical lows,  
558 the flow directions of intrusions within the Faroe-Shetland Sill Complex are also strongly  
559 controlled by the basement structure; in particular where basement bounding faults act as  
560 input points for intrusions into the Faroe-Shetland Basin (Schofield et al 2015). A close spatial  
561 relationship between several sills in the study area and the location of lava flows has been  
562 presented (e.g. Fig. 13) and it is proposed that the Faroe-Shetland Sill Complex sourced large  
563 parts of the volcanism described in this study. Because magma transport within basins tends  
564 to favour faults (Thomson and Schofield, 2008; Magee et al. 2013; Schofield et al. 2015), large  
565 parts of the Faroe-Shetland Basin volcanic succession were erupted on major highs like the  
566 Corona Ridge, raising the possibility that this area has substantial unimaged intrusions (e.g.  
567 Schofield et al. 2015). Due to the difficulty posed by intra and sub-basalt imaging, we cannot  
568 preclude that other sections of the Rosebank Field reservoirs are intruded, in particular by  
569 difficult to image sub-vertical dykes (Helland-Hansen, 2009, Schofield et al., 2015).

570

### 571 ***The Intra-Basaltic Play; a Restricted Play West of Shetland?***

572

573 Whilst the volcanic succession on the Corona Ridge has been shown to contain significant  
574 accumulations of petroliferous siliciclastic intra-basaltic sediments (Duncan et al. 2009), other  
575 intra-basaltic and supra-basaltic prospects drilled throughout the Faroe-Shetland Basin have  
576 so far proven to be less successful, leading to questions about the viability of the wider intra-  
577 basaltic play within the Faroe-Shetland Basin. A key uncertainty associated with the intra-  
578 basaltic play is understanding how siliciclastic sediments are transported into and dispersed  
579 throughout the volcanic succession.

580 The Súla intra-basaltic prospect, drilled by Statoil in 2014, is situated ~20 km north  
581 west of the Rosebank Field, in the Corona Basin. Although intra-basaltic sediments were

582 encountered they were not of prospective reservoir quality (P1847 Relinquishment Report).  
583 The 213/27-3 Rosebank North well faced a similar issue, situated ~6 km north of the  
584 Rosebank Main Field, with only poor quality sandstones encountered. In line with the  
585 palaeogeographic reconstructions presented in this paper (Fig. 17), areas north of the  
586 Rosebank Field are likely situated in a predominantly shelfal setting, outside of the play fairway  
587 that makes Rosebank viable.

588 A similar reduction in the quality and quantity of Colsay siliciclastic sands is noted to  
589 the south east of the Rosebank Field. The Aberlour prospect (214/28-1) tested the south-  
590 eastern extent of the Colsay sequence on the Corona Ridge. Although six Colsay sandstone  
591 intervals were encountered, they were thin and discrete, interbedded with volcanics and  
592 claystone sequences. Sandstone composition was typically quartzose, like Rosebank, however  
593 more fine grained. Further down dip, into the Flett Basin, intra-basaltic sediments are  
594 indicative of a deeper shelfal environment and are of poor reservoir quality (e.g. Tomintoul  
595 205/9-2). Consequently, given the reconstructed palaeoenvironment (Fig. 17), it is unlikely that  
596 significant quantities of clean sand were sourced from either the south east or the north of  
597 the basin. It is therefore necessary to invoke transport of sediment from the south west of  
598 the Rosebank Field. Here, the major T38/T40 erosional surface provides a record of a large  
599 sediment transfer event with palaeovalleys funnelling sediment into the Foinaven Sub-Basin,  
600 west of the Cambo High (Smallwood and Gill, 2002, Champion, M.E. *et al.*, 2008). Whilst fluvial  
601 sequences may be expected in this area (e.g. the sequence T40 204/18-1 fluvial sequence), the  
602 Anne-Marie prospect, drilled in 2010 ~15 km west of the Cambo High, encountered over 1  
603 km of volcanics before drilling was halted. This area of thickened volcanics would have acted  
604 as a barrier to intra-basaltic siliciclastic sediments. However, during periods of volcanic  
605 quiescence, diversion of fluvial sediments through the narrow corridor between Anne-Marie  
606 and the Cambo High could have provided a source of 'clean' sands in Rosebank. It should be



607 noted that the quality of sediment contained within these fluvial systems is questionable due  
608 to the deltaic to marginal marine facies they erode into (e.g. Longan 6005/15-1 as detailed by  
609 Morse, 2011).

610 Our findings suggest that the intra-basaltic play fairway within the Faroe-Shetland Basin  
611 is fairly narrow. A 30 × 30 km focal point for 'clean' intra-basaltic sands, comprising of the  
612 drainage system identified by Schofield & Jolley (2013) and another drainage system extending  
613 from Cambo to Rosebank, appear to represent the thickest accumulations of 'clean' intra-  
614 basaltic sands (Fig. 16). In terms of future potential exploration areas within the greater  
615 Cambo-Rosebank area, the identified drainage system located between Rosebank and Cambo  
616 potentially offers the best chance of success, in terms of reservoir risk, as this appears to be  
617 the system which supplied Rosebank with siliciclastic sand.

618 Towards the North of the Cambo structure, the same drainage system appears to  
619 onlap against the Cambo high (Fig. 16). Well 204/10a-5, was drilled in 2013 by Hess to appraise  
620 the down dip extent of the Colsay Member off the Cambo High (Fig. 16). The well intersected  
621 an 18 metre thick Colsay sequence, consisting of mudstone and a thin (~3 m) sand unit.  
622 However, inspecting the well location (Fig. 16), it appears the well was drilled on the very  
623 feather edge of the drainage system that extends between Cambo and Rosebank. Therefore,  
624 204/10a-5 was potentially not drilled in an optimum location to intersect a thick Colsay  
625 reservoir sequence. Colsay 1 and 3 sequences, which represent the main reservoir units in  
626 Rosebank, can be seen to thin and pinch against the Cambo high (Fig. 16C), forming the  
627 potential for a stratigraphic trap and separate hydrocarbon accumulation against the Cambo  
628 High. This pinch out is located ~500 m northwards of well 204/10a-5.

629

## 630 **Conclusions**

631

632 High quality seismic data sets have been integrated with well data to detail the controls on  
633 the distribution of volcanics and intra-basaltic sedimentation in the Cambo-Rosebank region  
634 of the Faroe-Shetland Basin. The structural setting of the Cambo-Rosebank region strongly  
635 controls both volcanism and sedimentation in the area. 'Clean' sands within the Rosebank  
636 Field are largely sourced from the southwest with the play fairway of the Rosebank Field  
637 restricted to the area surrounding the Corona Ridge. The volcanic sequences in Rosebank  
638 were erupted centrally within the basin, typically adjacent to, or on, structural weaknesses.  
639 Although the Rosebank play fairway seems to be spatially restricted, the Cambo-Rosebank  
640 region has significant exploration potential, particularly in zones of thickening adjacent to the  
641 southern Corona Ridge.

642

### 643 **Acknowledgments**

644 This paper forms part of a NERC Oil & Gas CDT PhD. PGS and TGS are thanked for donation  
645 of the FSB2011/12 MultiClient GeoStreamer® Survey without which this research would have  
646 been impossible. Stephen Morse is thanked for his constant input and support throughout the  
647 project. Chevron North Sea Limited are thanked for their interest and discussions on the  
648 Rosebank Field. All views, interpretations and opinion expressed in this article are entirely  
649 those of the authors and do not necessarily represent the views, interpretations or opinions  
650 of Chevron North Sea Limited. Jonathan Dietz is thanked for fieldwork in Iceland.

651

### 652 **References**

653

654 (2015, July) P1847 Relinquishment Report.

655 [https://itportal.ogauthority.co.uk/web\\_files/relinqs/nov2015/P1847.pdf](https://itportal.ogauthority.co.uk/web_files/relinqs/nov2015/P1847.pdf)

656

657 Baksi, A.K. 1987. Critical evaluation of the age of the Deccan Traps, India: Implications for  
658 flood-basalt volcanism and faunal extinctions. *Geology*, **15.2**, 147-150.

659

660 Beeson, M.H., Terry L.T. & James L.A. 1989. The Columbia River Basalt Group in western  
661 Oregon; geologic structures and other factors that controlled flow emplacement  
662 patterns. *Geological Society of America Special Papers*, **239**, 223-246.

663

664 Boldreel, L.O. 2006. Wire-line log-based stratigraphy of flood basalts from the Lopra-I/IA  
665 well, Faroe Islands. *Geological Survey of Denmark and Greenland Bulletin*, **9**, 7-22.

666

667 Champion, M.E., White, N.J., Jones, S.M. and Lovell, J.P.B., 2008. Quantifying transient mantle  
668 convective uplift: An example from the Faroe-Shetland basin. *Tectonics*, **27**, (1).

669

670 Coney, D., Fyfe, T.B., Retail, P. & Smith, P.J. 1993. Clair appraisal: the benefits of a co-operative  
671 approach. *Geological Society, London, Petroleum Geology Conference series*, **4**, 1409-1420.

672

673 Van Dedem, E.J. and Verschuur, D.J., 1998. 3D surface-related multiple elimination and interpolation.  
674 In *SEG Technical Program Expanded Abstracts*. Society of Exploration Geophysicists. 1321-1324

675

676 Day, A., Klüver, T., Söllner, W., Tabti, H. and Carlson, D., 2013. Wavefield-separation methods for dual-  
677 sensor towed-streamer data. *Geophysics*, **78**, 55-70.

678

679 Dean, K. McLachlan, K. & Chambers, A. 1999. Rifting and the development of the Faeroe-  
680 Shetland Basin. *Geological Society, London, Petroleum Geology Conference series*, **5**, 533-544.  
681

682 Doré, A. G., Lundin, E.R., Fichler, C. & Olesen, O. 1997 Patterns of basement structure and  
683 reactivation along the NE Atlantic margin. *Journal of the Geological Society*, **154.1**, 85-92.  
684

685 Doré, A. G., Lundin, E.R., Jensen, L.N., Birkeland, Ø., Eliassen, P.E. & Fichler, C. 1999. "Principal  
686 tectonic events in the evolution of the northwest European Atlantic margin." *Geological society,*  
687 *London, petroleum geology conference series*, **5**, 41-61.  
688

689 Duindam, P. & Van Hoorn, B. 1987. Structural evolution of the West Shetland continental  
690 margin. *Petroleum Geology of North West Europe. Graham and Trotman*, **2**, 765-773.  
691

692 Duncan, L., Helland-Hansen, D. & Dennehy, C. 2009. The Rosebank Discovery, A new play  
693 type in intra basalt reservoirs of the North Atlantic volcanic province. *In: 6th European*  
694 *Production and Development Conference and Exhibition (DEVEX), Abstracts. Chevron Upstream*  
695 *Europe, Aberdeen. [http://www.devex-conference.org/Presentations\\_2009/](http://www.devex-conference.org/Presentations_2009/).*  
696

697 Ebdon, C.C., Granger, P.J., Johnson, H.D. and Evans, A.M., 1995. Early Tertiary evolution and  
698 sequence stratigraphy of the Faeroe-Shetland Basin: implications for hydrocarbon  
699 prospectivity. *Geological Society, London, Special Publications*, **90(1)**, 51-69.  
700

701 Ebinghaus, A., Hartley, A.J., Jolley, D.W., Hole, M. and Millett, J., 2014. Lava–Sediment  
702 Interaction and Drainage-System Development in a Large Igneous Province: Columbia River

703 Flood Basalt Province, Washington State, USA. *Journal of Sedimentary Research*, **84(11)**, 1041-  
704 1063.

705

706 Ellis, D., Bell, B.R., Jolley, D.W. & O'Callaghan, M. 2002. The stratigraphy, environment of  
707 eruption and age of the Faroes Lava Group, NE Atlantic Ocean. *Geological Society, London,*  
708 *Special Publications*, **197.1**, 253-269.

709

710 Ellis, D., Jolley, D.W., Passey, S.R. and Bell, B.R. 2009. Transfer zones: The application of new  
711 geological information from the Faroe Islands applied to the offshore exploration of intra  
712 basalt and sub-basalt strata. In: Ziska, H. and Varming, T. (eds) Faroe Islands Exploration  
713 Conference: Proceedings of the

714

715 Gawthorpe, R. L., and Hurst, J.M. 1993 Transfer zones in extensional basins: their structural  
716 style and influence on drainage development and stratigraphy. *Journal of the Geological*  
717 *Society*, **150.6**, 1137-1152.

718

719 Gilani, S.F., and Gómez-Martínez, L. 2015 The application of data conditioning, frequency  
720 decomposition and RGB colour blending in the Gohta discovery (Barents Sea, Norway). *First*  
721 *Break*, **33.12**, 39-45.

722

723 Hargreaves, N. and Cooper, N., 2001. High-resolution Radon demultiple. In *SEG Technical Program*  
724 *Expanded Abstracts*. Society of Exploration Geophysicists. 1325-1328.

725

726 Hartley, R.A., et al. 2011 Transient convective uplift of an ancient buried landscape. *Nature*  
727 *Geoscience*, **4.8**, 562-565.

728

729 Helland-Hansen, D. 2009. Rosebank—challenges to development from a subsurface  
730 perspective. *Faroe Islands Exploration Conference, 2nd Conference Annales Societatis Scientiarum,*  
731 *Proceedings, Supplementum, 50.*

732

733 Jerram, D.A. & Widdowson, M. 2005. The anatomy of Continental Flood Basalt Provinces:  
734 geological constraints on the processes and products of flood volcanism. *Lithos, 79(3), 385-*  
735 *405.*

736

737 Jolley, D.W., Passey, S.R., Hole, M. & Millett, J. 2012. Large-scale magmatic pulses drive plant  
738 ecosystem dynamics. *Journal of the Geological Society, 169.6, 703-711.*

739

740 Jolley, D.W. & Widdowson, M. 2005. Did Paleogene North Atlantic rift-related eruptions  
741 drive early Eocene climate cooling? *Lithos, 79.3, 355-366.*

742

743 Kimbell, G.S., Tichie, J.D., Johnson, H. & Gatliff, R.W. 2005. Controls on the structure and  
744 evolution of the NE Atlantic margin revealed by regional potential field imaging and 3D  
745 modelling. *Geological Society, London, Petroleum Geology Conference series, 6, Geological Society*  
746 *of London.*

747

748 Knox, R.W.O.B., Holloway, S., Kirby, G.A. & Bailey, H.E. 1997 Stratigraphic nomenclature of  
749 the UK North West Margin. 2. Early Paleogene Lithostratigraphy and Sequence Stratigraphy.  
750 *British Geological Survey, Nottingham.*

751

752 Kristiansen, P., Fowler, P. and Mobley, E., 2003. Anisotropic Kirchhoff prestack time migration for  
753 enhanced multicomponent imaging. In *SEG Technical Program Expanded Abstracts*. Society of  
754 Exploration Geophysicists. 961-964.

755

756 Lamers, E., & Carmichael, S.M.M. 1999. The Paleocene deepwater sandstone play west of  
757 Shetland. *Geological Society, London, Petroleum Geology Conference series*, **5**.

758

759 Magee, C., Jackson, C.A.L., & Schofield, N. 2013. The influence of normal fault geometry on  
760 igneous sill emplacement and morphology. *Geology*, **41.4**, 407-410.

761

762 Magee, C., Hunt-Stewart, E. & Jackson, C.A.L. 2013. Volcano growth mechanisms and the role  
763 of sub-volcanic intrusions: Insights from 2D seismic reflection data. *Earth and Planetary Science*  
764 *Letters*, **373**, 41-53.

765

766 Millett, J.M., Hole, M.J. & Jolley, D.W. 2014. A fresh approach to ditch cutting analysis as an  
767 aid to exploration in areas affected by large igneous province (LIP) volcanism. *Geological Society,*  
768 *London, Special Publications*, **397(1)**, 193-207.

769

770 Millett, J. M., Hole, M.J., Jolley, D.W., Schofield, N. & Campbell, E. 2016. "Frontier exploration  
771 and the North Atlantic Igneous Province: new insights from a 2.6 km offshore volcanic  
772 sequence in the NE Faroe–Shetland Basin." *Journal of the Geological Society*, **173.2**, 320-336.

773

774 Morse, S.J. 2013. The Supply of Siliclastic Input to Potential Late Paleocene Sub-Basaltic  
775 Reservoirs in the Faroe Shetland Basin. *Thesis for: Msc Petroleum Geoscience, Royal Holloway*  
776 *University*

777 Moy, D. J., & Imber, J. 2009. A critical analysis of the structure and tectonic significance of rift-  
778 oblique lineaments ('transfer zones') in the Mesozoic–Cenozoic succession of the Faroe–  
779 Shetland Basin, NE Atlantic margin. *Journal of the Geological Society*, **166.5**, 831-844.

780

781 Nelson, C.E., Jerram D.A., & Hobbs, R.W. 2009. Flood basalt facies from borehole data:  
782 implications for prospectivity and volcanology in volcanic rifted margins. *Petroleum*  
783 *Geoscience*, **15.4**, 313-324.

784

785 Passey, S.R. & Bell, B.R. 2007. Morphologies and emplacement mechanisms of the lava flows  
786 of the Faroe Islands Basalt Group, Faroe Islands, NE Atlantic Ocean. *Bulletin of Volcanology*,  
787 **70.2**, 139-156.

788

789 Passey, S.R. & Jolley, D.W., 2008. A revised lithostratigraphic nomenclature for the Palaeogene  
790 Faroe Islands Basalt group, NE Atlantic Ocean. *Earth and Environmental Science Transactions of*  
791 *the Royal Society of Edinburgh*, **99(3-4)**, 127-158.

792 Poppitt, S., Duncan, L.J., Preu, B., Fazzari, F. and Archer, J., 2016, December. The influence of  
793 volcanic rocks on the characterization of Rosebank Field—new insights from ocean-bottom  
794 seismic data and geological analogues integrated through interpretation and modelling. In  
795 *Geological Society, London, Petroleum Geology Conference series (Vol. 8, pp. PGC8-6)*. Geological  
796 Society of London.

797



798 Rasmussen, J. & Noe-Nygaard, A. 1970 Geology of the Faeroe Islands: (pre-quaternary).  
799

800 Reidel, S.P., Camp, V.E. & Tolan, T.L. 2013. The Columbia River flood basalt province:  
801 Stratigraphy, areal extent, volume, and physical volcanology. *Geological Society of America*  
802 *Special Papers*, **497**, 1-43.  
803

804 Reidel, S.P. & Hooper, P.R. 1989 *Volcanism and tectonism in the Columbia River flood-basalt*  
805 *province*. Vol. 239. Geological Society of America.  
806

807 Ritchie, J. D., Ziska, H., Johnson, H. & Evans, D. 2011 Geology of the Faroe-Shetland Basin  
808 and adjacent areas.  
809

810 Schofield, N. & Jolley, D.W. 2013. Development of intra-basaltic lava-field drainage systems  
811 within the Faroe–Shetland Basin. *Petroleum Geoscience*, **19(3)**, 273-288.  
812

813 Schofield, N., Holford, S., Millett, J., Brown, D., Jolley, D., Passey, S.R., Muirhead, D., Grove,  
814 C., Magee, C., Murray, J. & Hole, M. 2015. Regional magma plumbing and emplacement  
815 mechanisms of the Faroe-Shetland Sill Complex: implications for magma transport and  
816 petroleum systems within sedimentary basins. *Basin Research*.  
817

818 Smallwood, J.R. & Gill, C.E. 2002. The rise and fall of the Faroe–Shetland Basin: evidence from  
819 seismic mapping of the Balder Formation. *Journal of the Geological Society*, **159.6**, 627-630.  
820

821 Spitzer, R., White, R.S. & Christie, P.A.F. 2008. Seismic characterization of basalt flows from  
822 the Faroes margin and the Faroe-Shetland basin. *Geophysical Prospecting*, **56.1**, 21-31.

823

824 Varming, T., Ziska, H. & Ólvasdóttir, J. 2012. Exploring for hydrocarbons in a volcanic  
825 province—A review of exploration on the Faroese Continental Shelf. In *Faroe Islands*  
826 *Exploration Conference: Proceedings of the 3rd Conference. Annales Societatis Scientiarum, Færoensis,*  
827 *Supplementum*, **56**, 84-106.

828

829 Waagstein, R. 1988. Structure, composition and age of the Faeroe basalt plateau. *Geological*  
830 *Society, London, Special Publications*, **39(1)**, 225-238.

831

832 Walker, G.P.L. 1971. Compound and simple lava flows and flood basalts. *Bulletin*  
833 *Volcanologique*, **35(3)**, 579-590.

834

835 Watson, D., Schofield, N., Jolley, D., Archer, S., Finlay, A.J., Mark, N., Hardman, J. and Watton,  
836 T., 2017. Stratigraphic overview of Palaeogene tuffs in the Faroe–Shetland Basin, NE Atlantic  
837 Margin. *Journal of the Geological Society*, pp.jgs2016-132.

838

839 Wells, S.G., Dohrenwend, J.C., McFadden, L.D., Turrin, B.D. & Mahrer K.D. 1985 Late  
840 Cenozoic landscape evolution on lava flow surfaces of the Cima volcanic field, Mojave Desert,  
841 California. *Geological Society of America Bulletin*, **96.12**, 1518-1529.

842

843 White, R.S., Smallwood, J.R., Fliedner, M.M., Boslaugh, B., Maresh, J. & Fruehn, J. 2003. Imaging  
844 and regional distribution of basalt flows in the Faeroe-Shetland Basin. *Geophysical*  
845 *Prospecting*, **51.3**, 215-231.

846

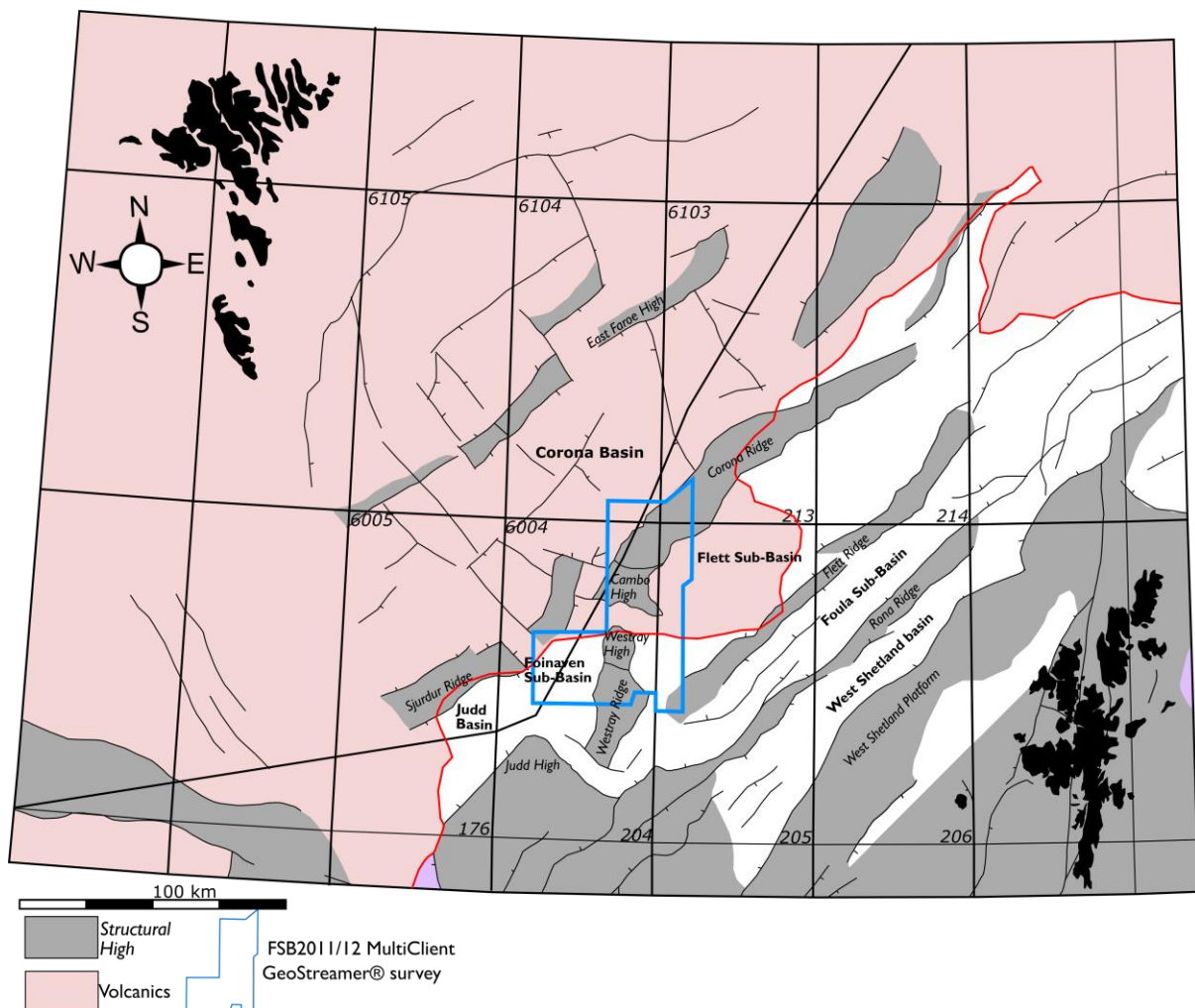
847 Ziolkowski, A., Hanssen, P., Gatliff, R., Jakubowicz, H., Dobson, A., Hampson, G., Li, X. & Liu,  
848 E. 2003. Use of low frequencies for sub-basalt imaging. *Geophysical Prospecting*, **51.3**, 169-182.

849

850

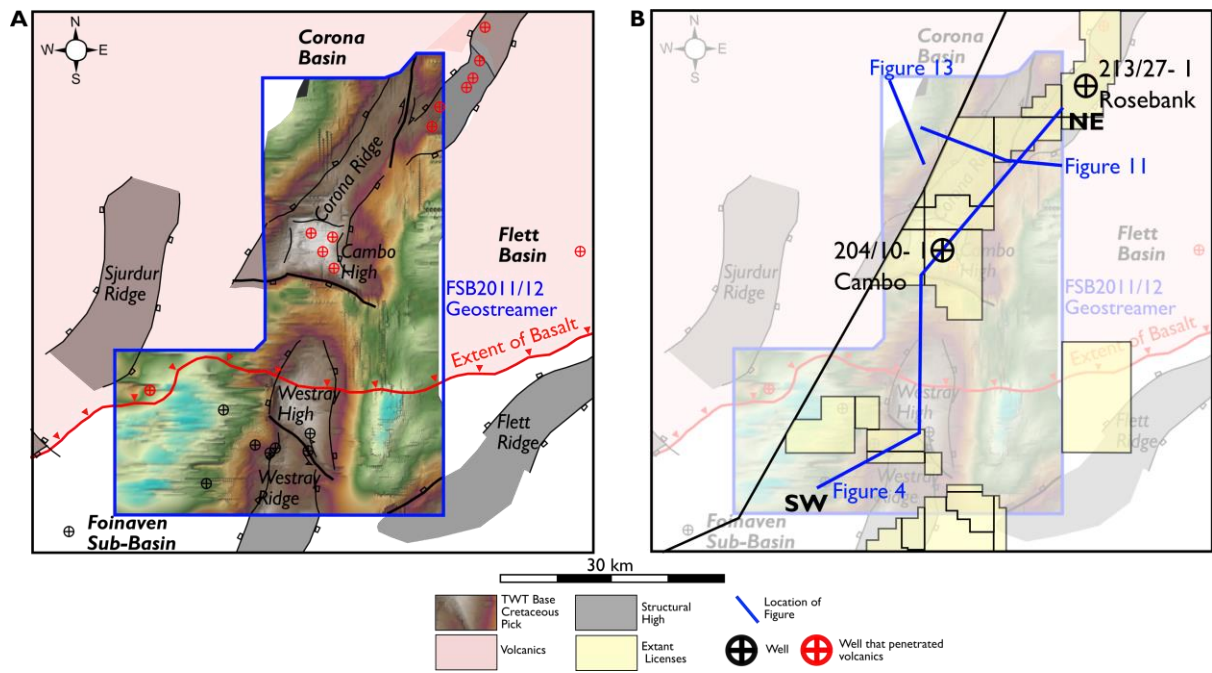
851

852 **Figure Captions**



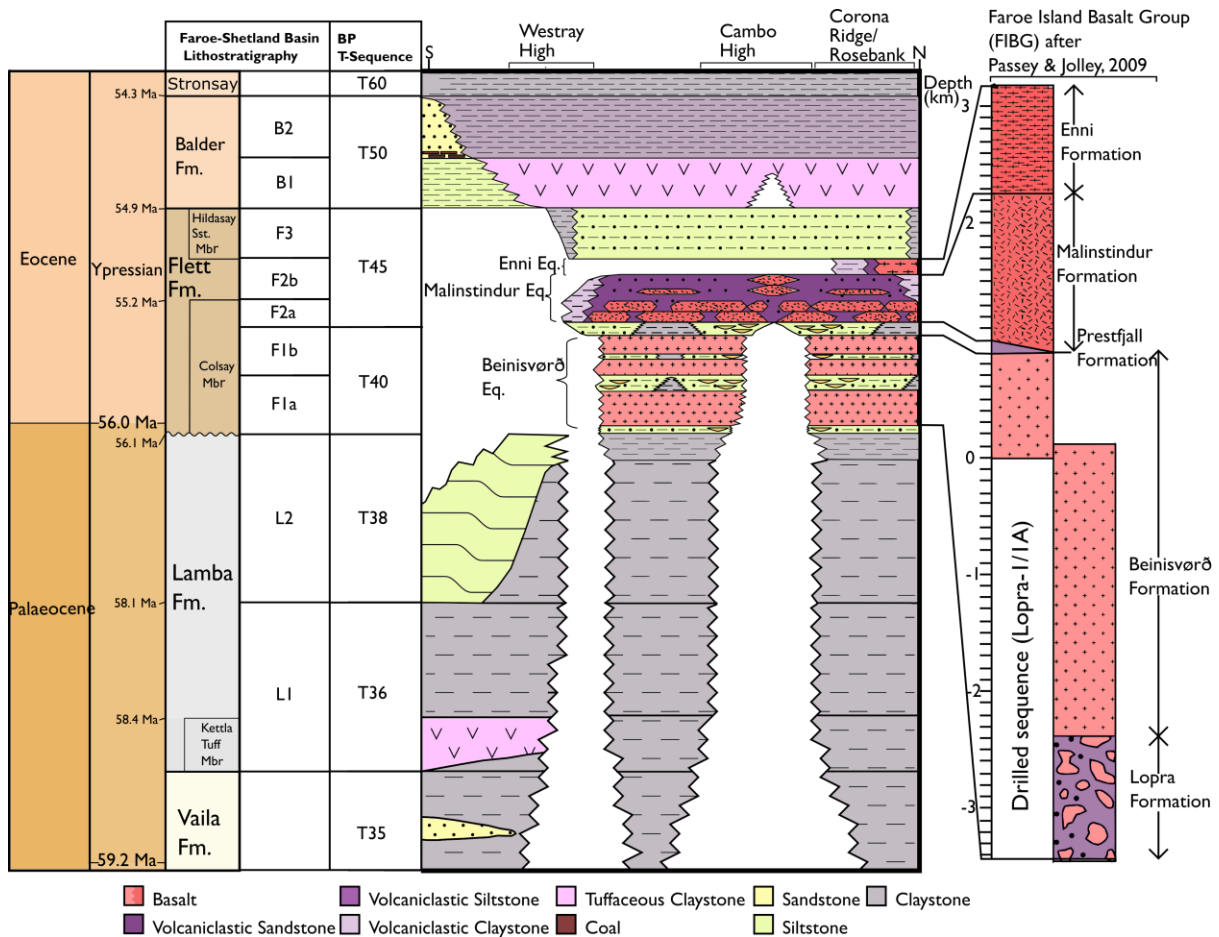
853

854 **Fig 1.** Map of the Faroe-Shetland Basin highlighting main structural highs and the areal  
855 extent of Upper Palaeocene/Lower Eocene volcanics. Modified from Moy (2009). Outline of  
856 the FSB2011/12 Multiclient Geostreamer® survey included.



857

858 **Fig 2.** (a) Plan view of the FSB2011/12 Multiclient Geostreamer® survey including TWT  
 859 map of the base Cretaceous. Main structural elements of the study area are shown as well  
 860 as the extent of the basalt cover. Outline of seismic coverage and wells used within the  
 861 study shown. (b) Outline of currently extent licenses within the study area. Location of later  
 862 figures highlighted.



863

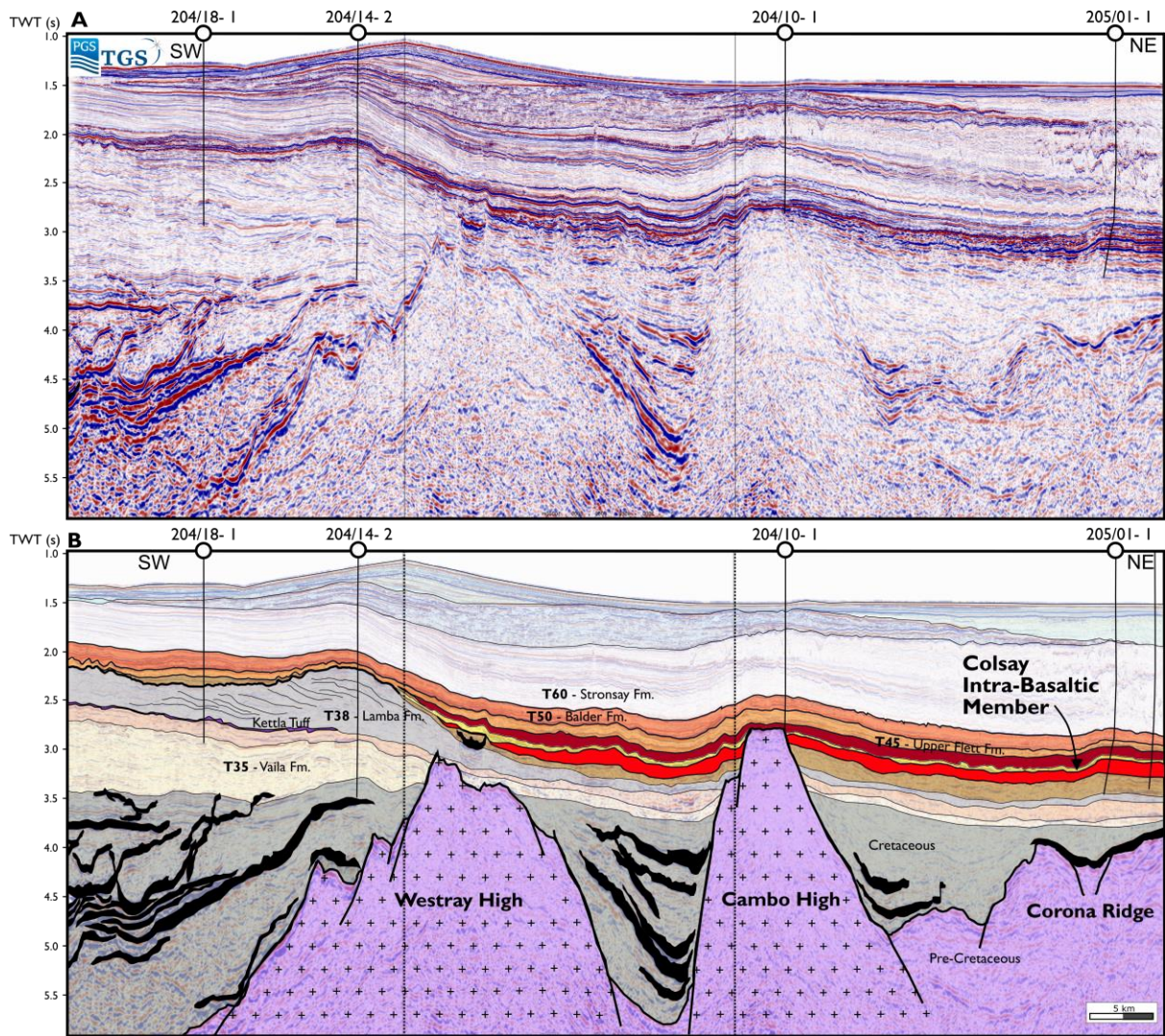
864

865

866

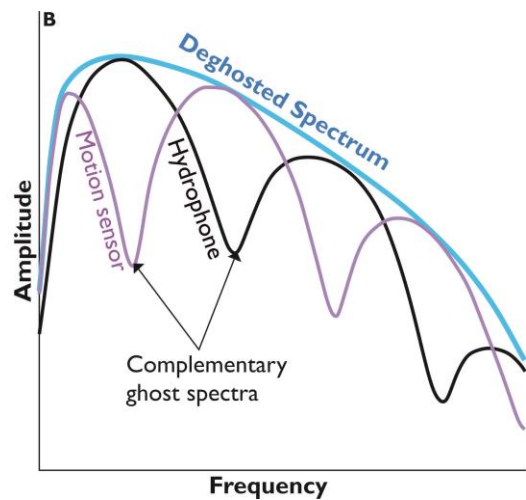
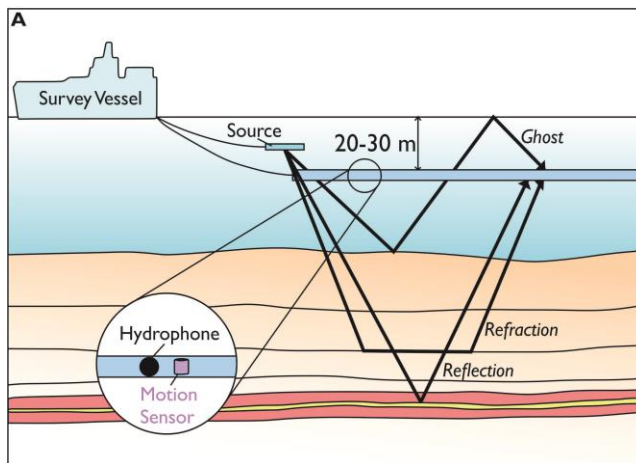
867

**Fig 3.** Chronostratigraphic chart of the Upper Palaeocene and Lower Eocene of the study area incorporating BP's T-sequence scheme (Ebdon *et al.*, 1995) with the lithostratigraphy of Ritchie (2011). The relative stratigraphical position of the Faroe Islands Basalt Group is shown after Passel & Jolley, 2009.



868

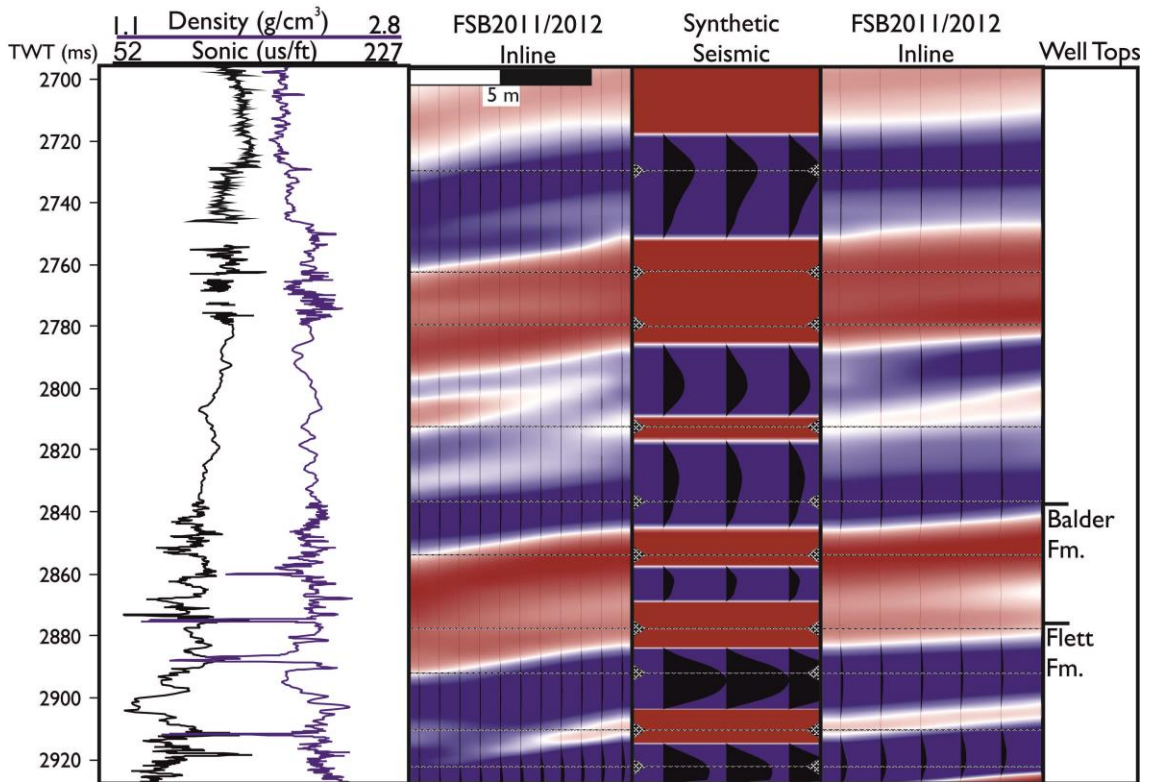
869 **Fig 4.** (a) Uninterpreted regional seismic line of the study area. Data courtesy of PGS (the  
 870 FSB201 I/12 MultiClient GeoStreamer® survey) (b) Interpreted regional seismic line of the  
 871 study area highlighting the Upper Palaeocene/ Lower Eocene succession. Key geological  
 872 features referred to in the text highlighted in bold.



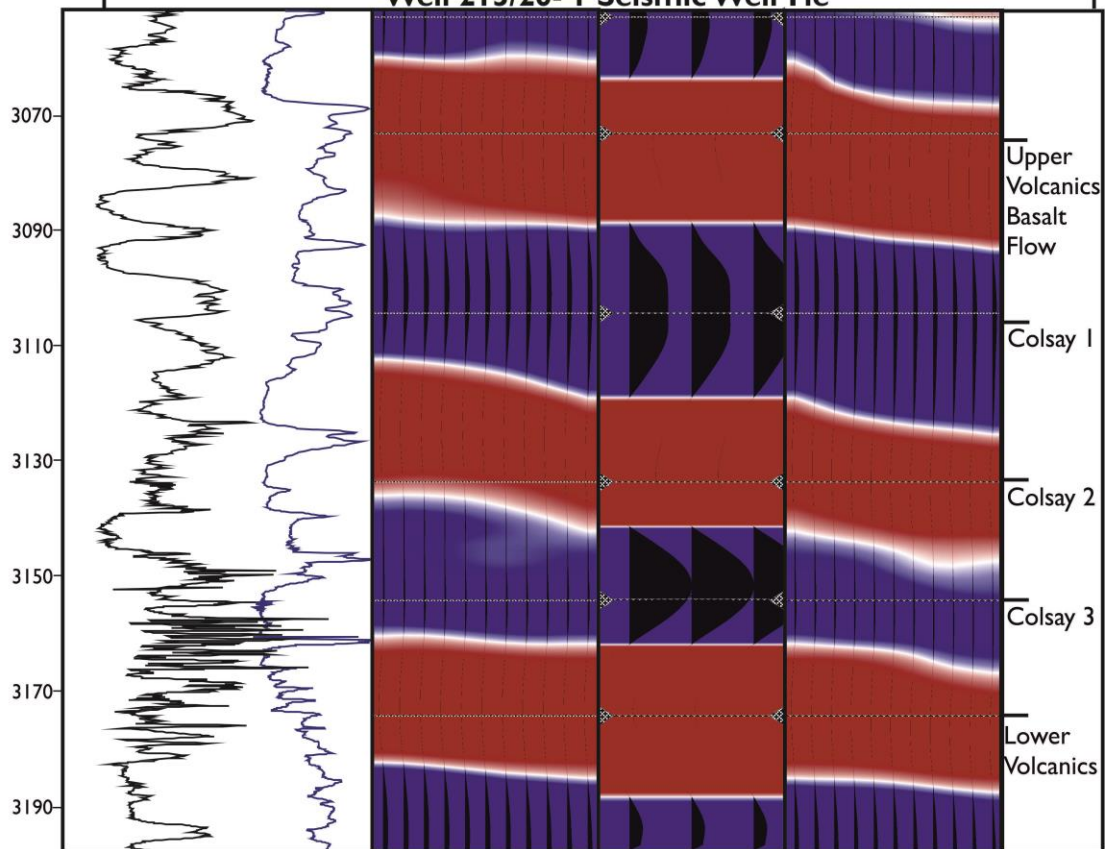
873

874 **Fig. 5** Outline of the Geostreamer<sup>®</sup> technology used during the acquisition of the  
875 FSB2011/2012 Survey. **A** Graphic detailing the depth at which the streamer is towed, the  
876 dual sensors used during acquisition of the data, and the principle behind the ghost  
877 reflection within seismic data. **B** Graph used to indicate the principle behind the deghosting  
878 of the Geostreamer data. The hydrophone and motion sensor record complementary ghost  
879 spectra that, when summed, eliminate gaps within the frequency gaps within the seismic  
880 data.

**Well 205/01- I Seismic Well Tie**

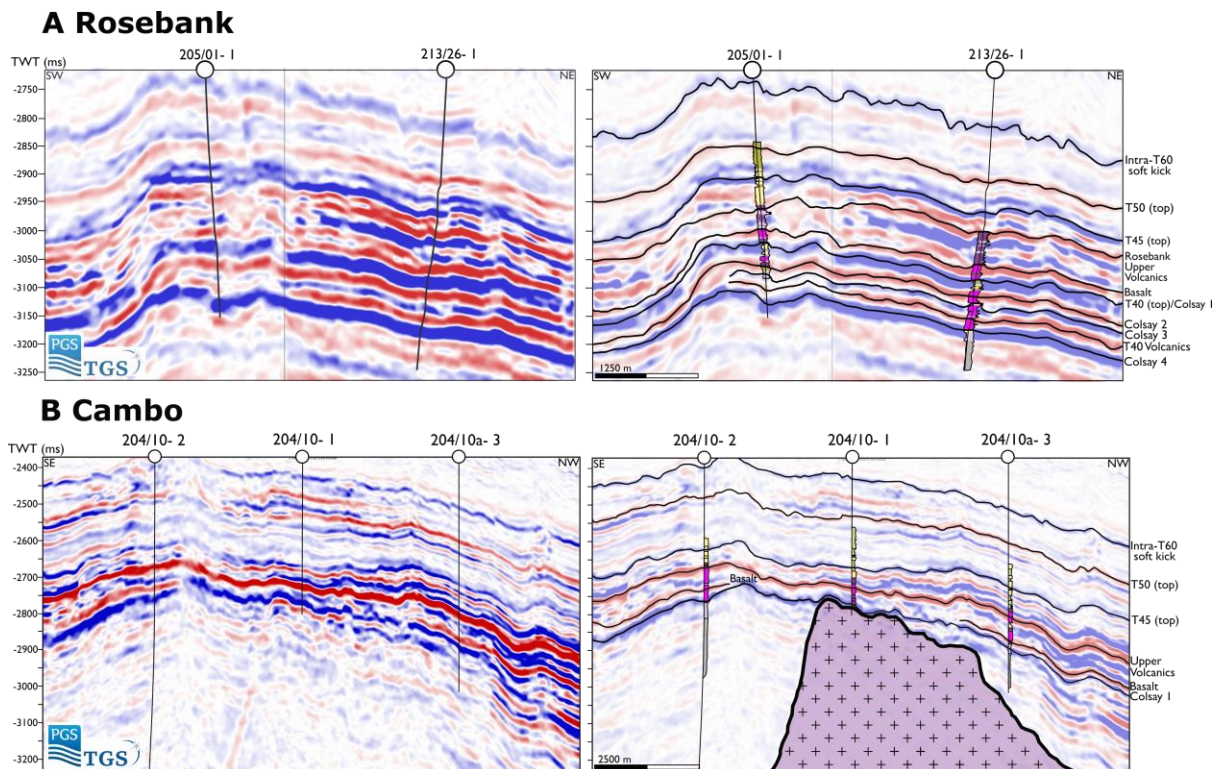


**Well 213/26- I Seismic Well Tie**

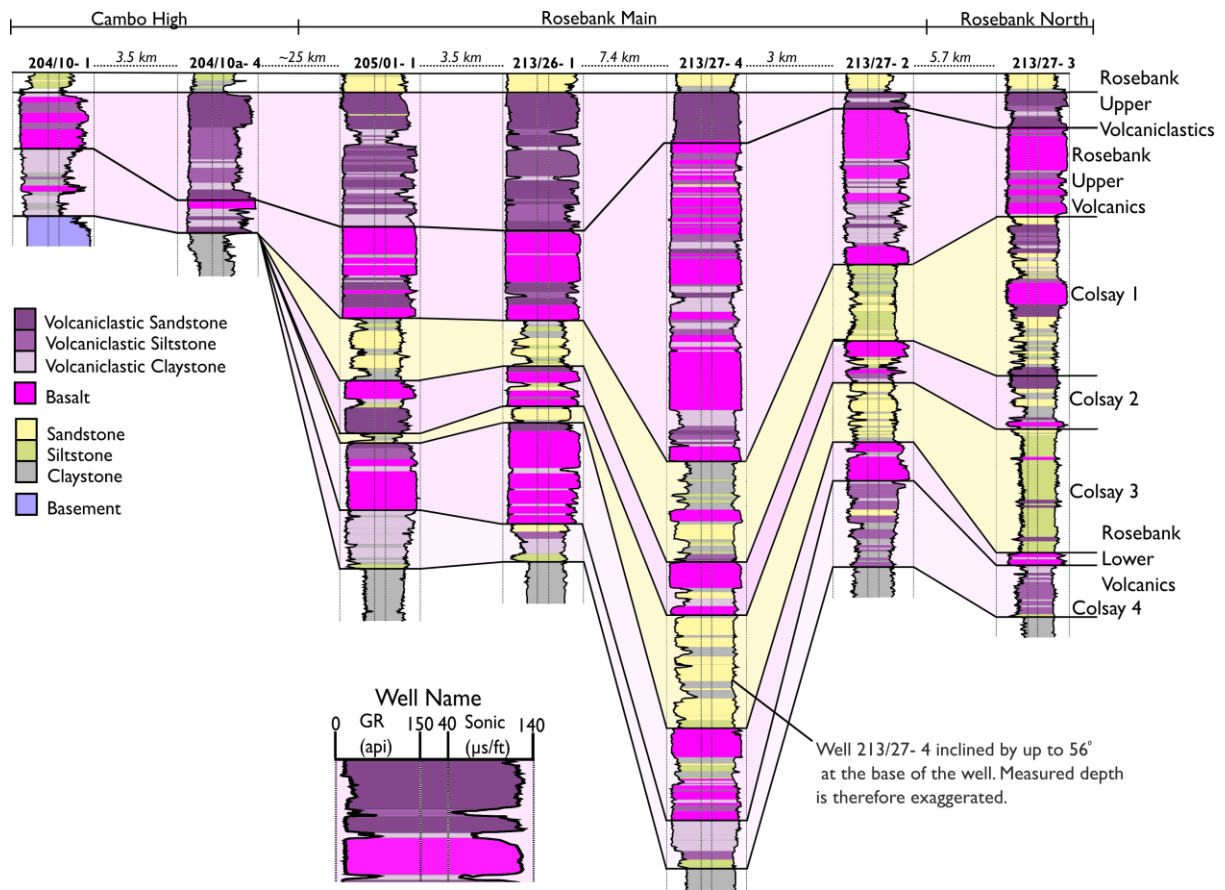




882 **Fig. 6** Seismic well tie for the Rosebank wells within the Geostreamer. The 205/01- 1 well  
 883 is used to demonstrate the fit between the well logs and FSB 2011/2012 survey in the post-  
 884 volcanic succession. The 213/26- 1 well is used to demonstrate the close fit between the  
 885 well data throughout the volcanic succession. Synthetic seismic was generated in Petrel  
 886 using a combination of sonic and density wireline data. A volcanic succession well tie for the  
 887 205/01- 1 well is not shown due to the lack of density data throughout the Rosebank Upper  
 888 Volcaniclastics.

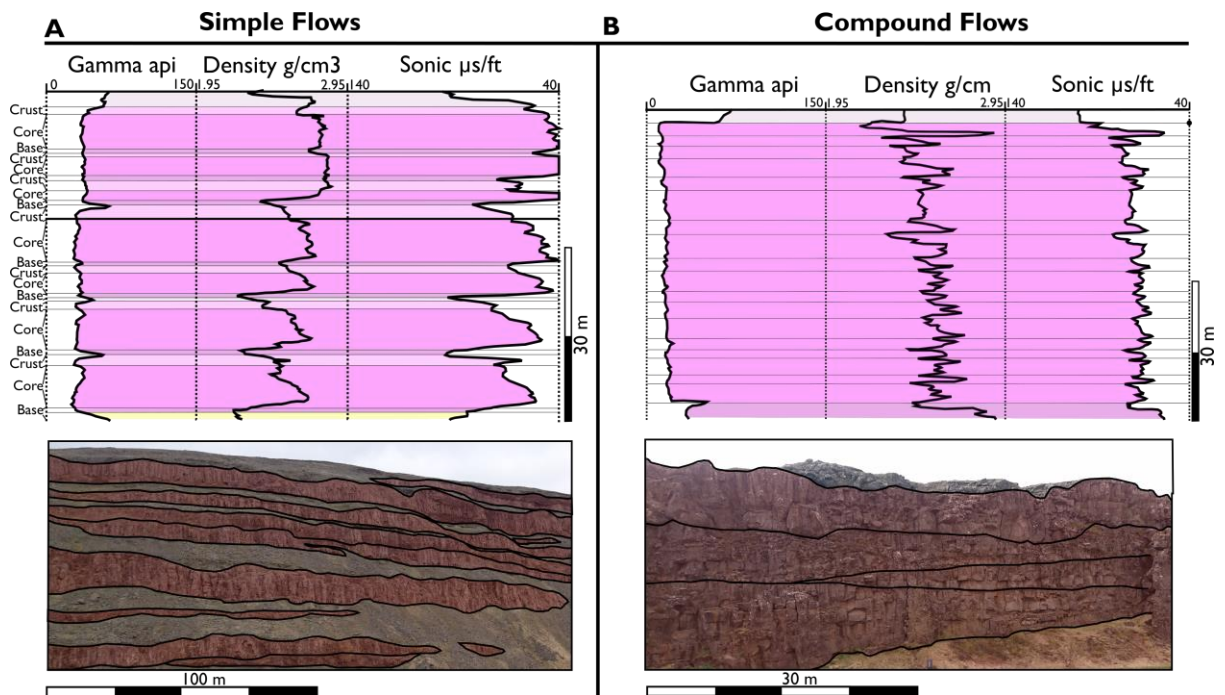


889  
 890 **Fig 7.** Interpreted and uninterpreted seismic lines of the **A** Cambo High and **B** southern  
 891 Rosebank wells highlighting key geological horizons within and above the volcanic  
 892 succession. Data courtesy of PGS (the FSB2011/12 MultiClient GeoStreamer® survey)



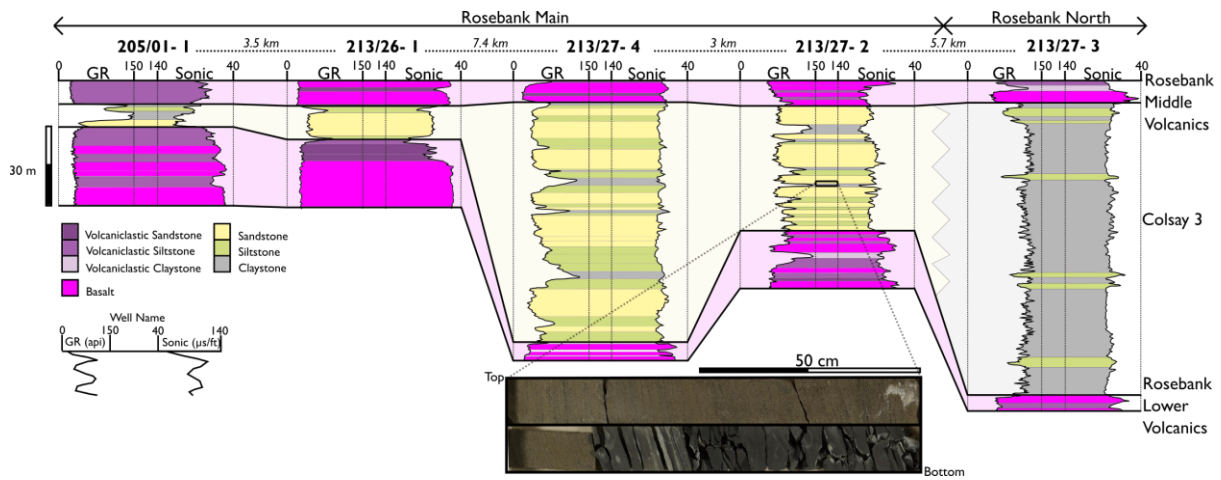
893

894 **Fig. 8** Well correlation of the entire volcanic succession throughout the Rosebank field,  
 895 joined to wells from the Cambo field, 25 km to the southwest. Well 213/27- 4 is highly  
 896 deviated resulting in an exaggerated measured depth.

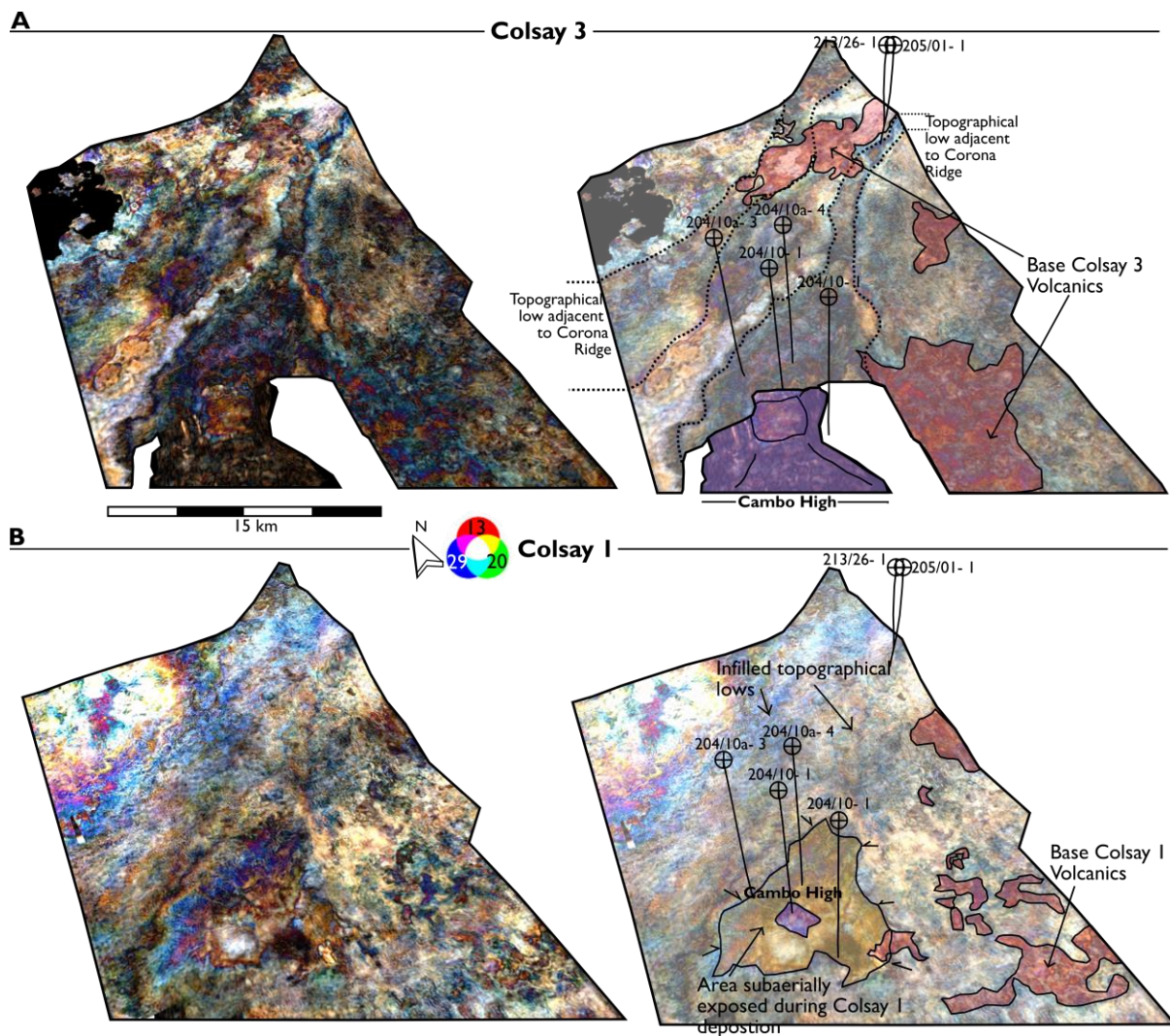


897

898 **Fig 9.** Petrophysical, seismic and outcrop expression of **A** simple and **B** compound lava  
 899 flows. Petrophysical logs taken from the 213/26- I Rosebank Well. Photos taken on Iceland.

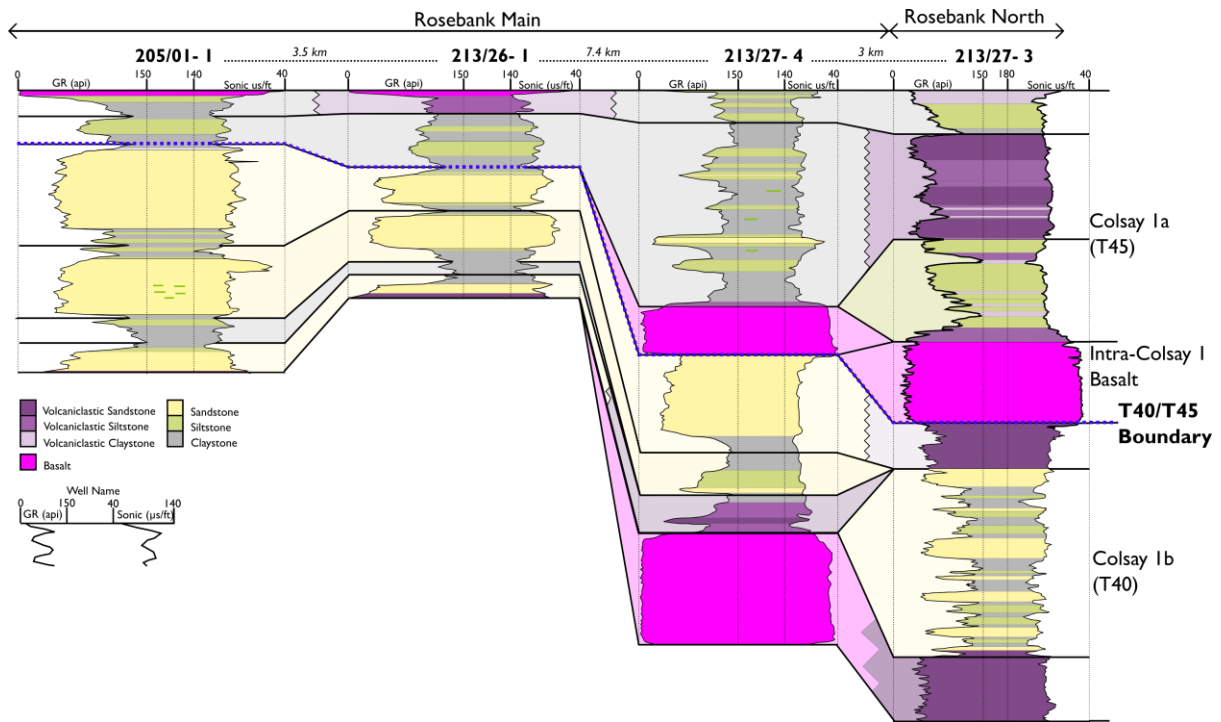


900  
 901 **Fig 10.** Well correlation of the Colsay 3 package through 5 of the Rosebank Wells, SW to  
 902 NE along the Corona Ridge. Conventional core and its location within the 213/27- 2 well is  
 903 shown. Detailed description of Colsay 3 is provided within the text.

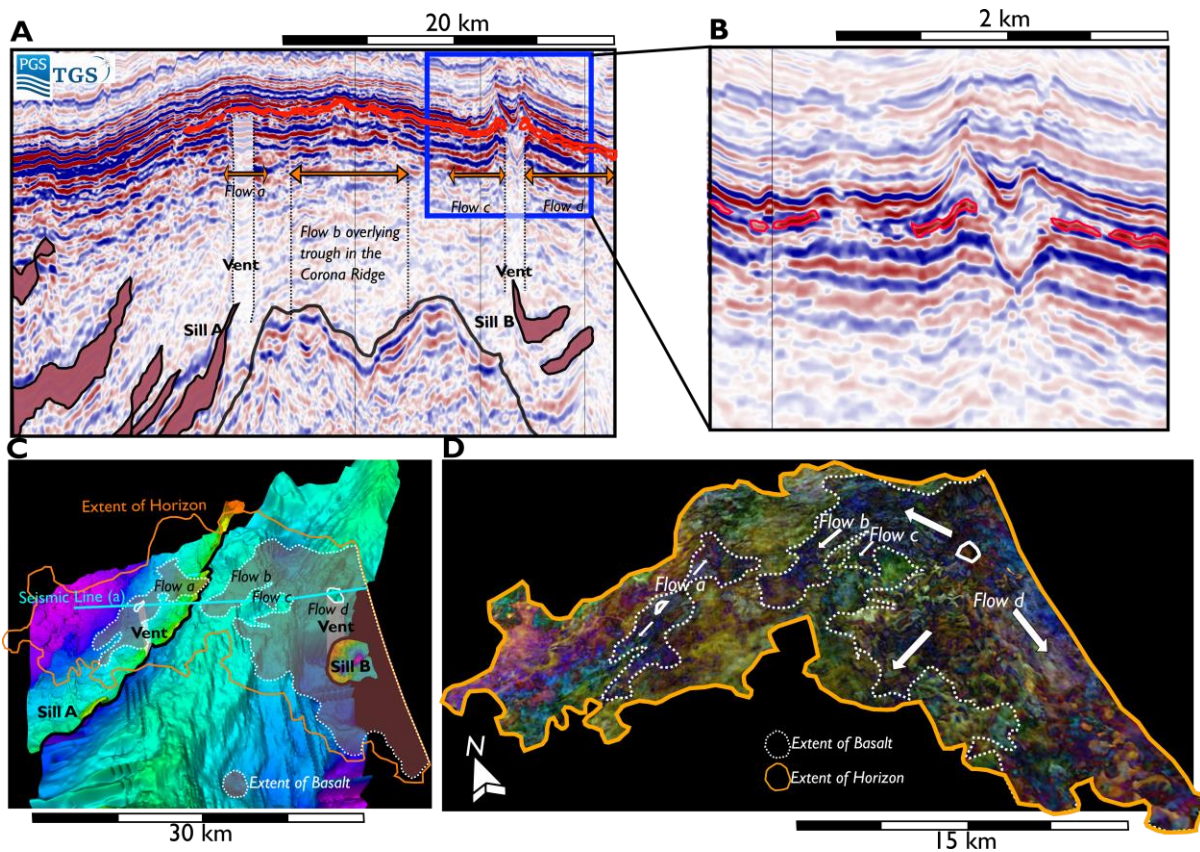


904

905 **Fig 11.** RGB frequency spectral decompositions carried out on Colsay I and Colsay 3  
 906 horizons mapped within the Faroe-Shetland Basin 2011/12 Geostreamer® Survey Spectral  
 907 decompositions of **A** Colsay 3 and **B** Colsay I seismic horizons. Spectral decompositions  
 908 were carried out within GeoTeric. Interpreted horizons highlight key features described in  
 909 the text.



910  
 911 **Fig 12.** Well correlation of the Colsay I package through 4 of the Rosebank Wells, SW to  
 912 NE along the Corona Ridge. Detailed description of Colsay I is provided within the text.



913

914

915

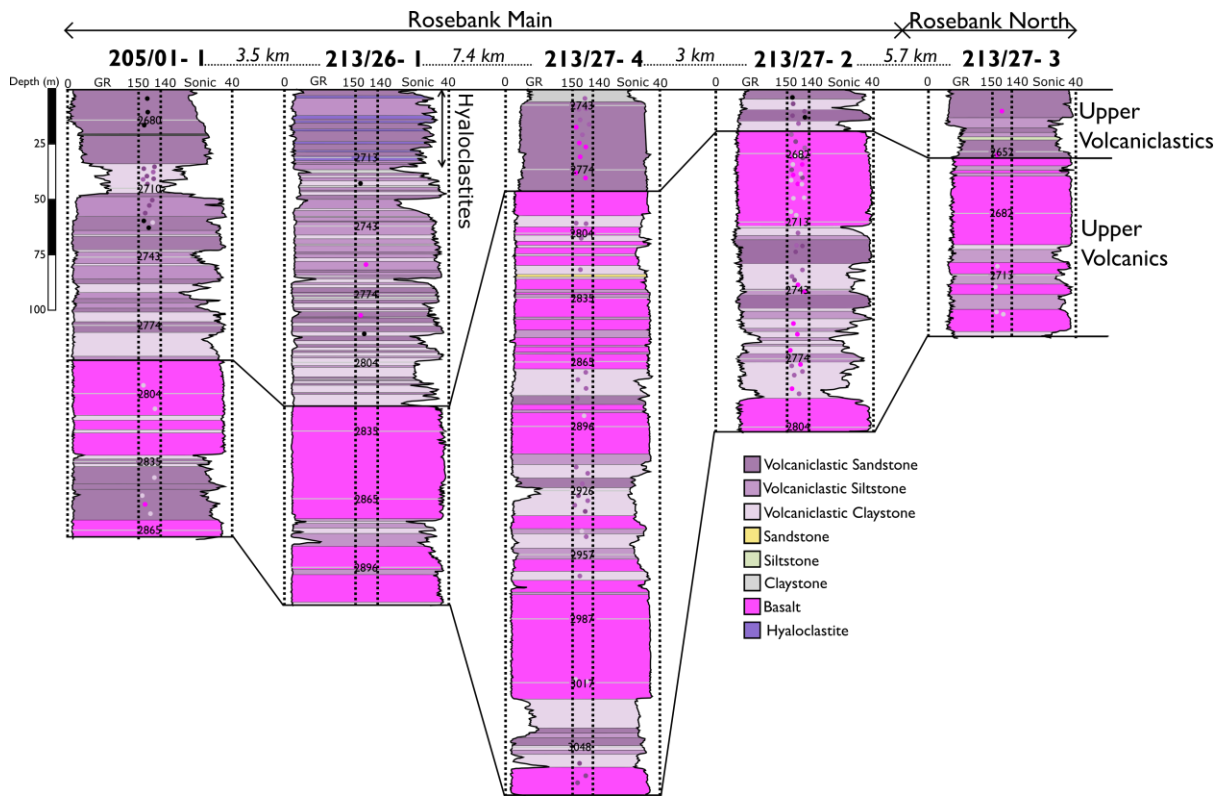
916

917

918

919

**Fig 13. A** Interpreted seismic line across the Corona Ridge highlighting the Rosebank Upper Volcanics seismic horizon, the Corona Ridge and the location of igneous intrusions. **B** Inset of a highlighting major vent structure and the seismic character of the Rosebank Upper Volcanics. **C** Location of major features overlying a TWT map of the base Cretaceous. **D** Spectral decomposition of the Rosebank Upper Volcanics seismic horizon showing the outline and flow direction of lava flows.

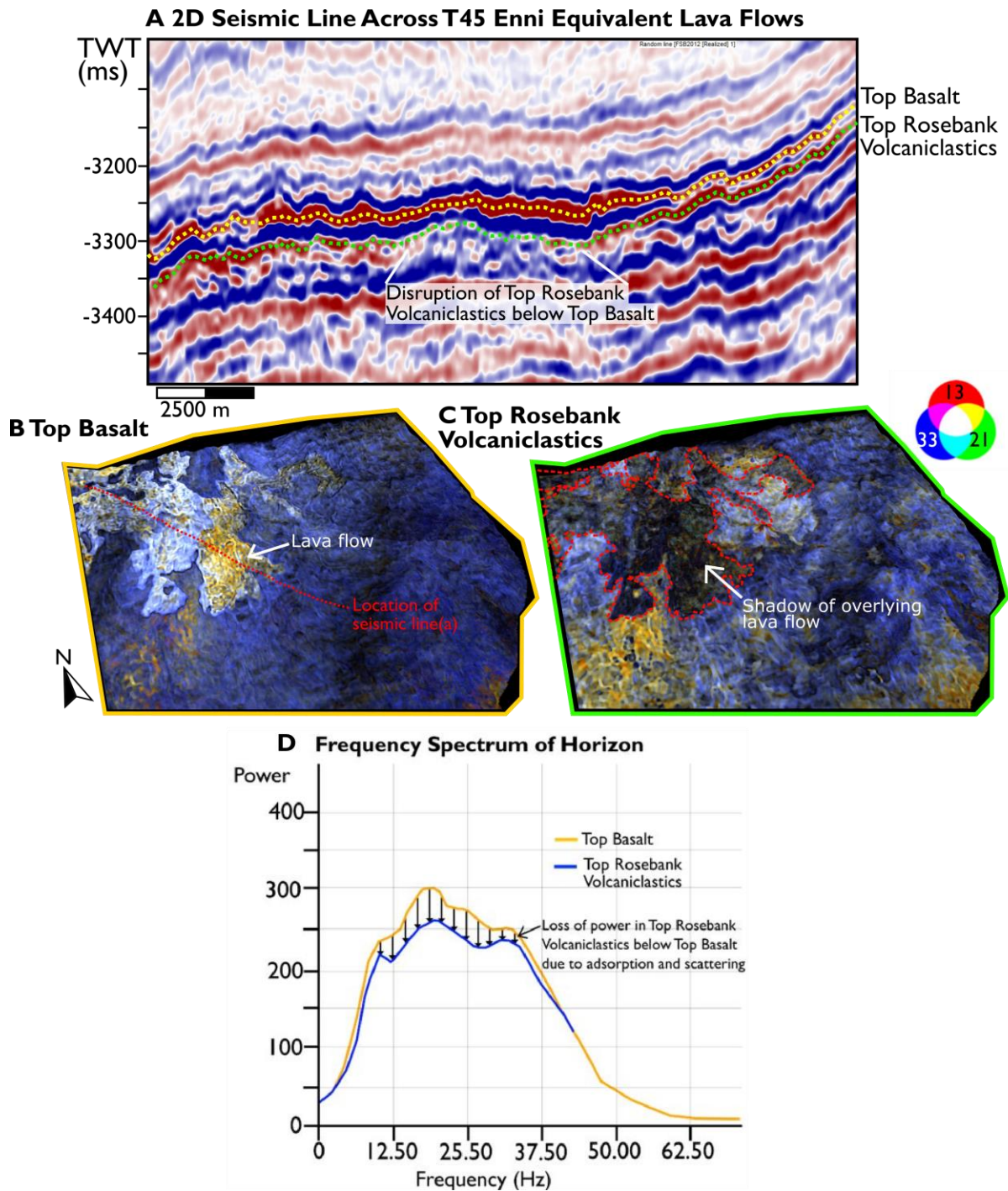


920

921 **Fig 14.** Well Correlation of the Rosebank Upper Volcanics package and the Rosebank

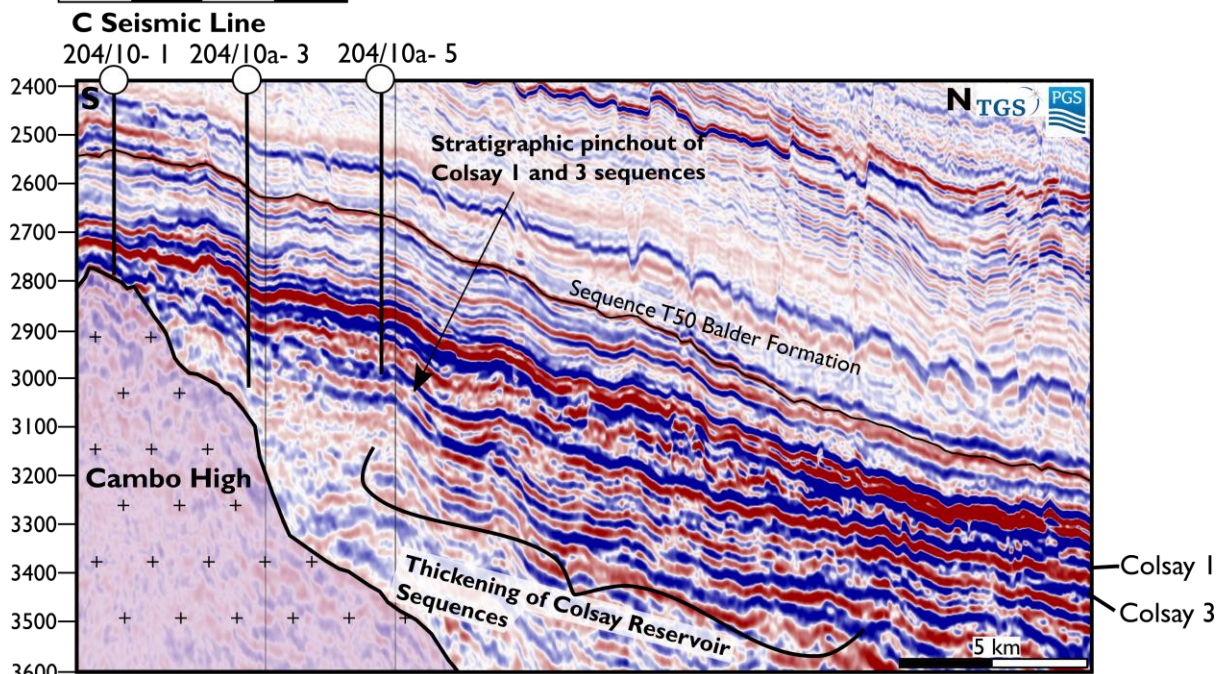
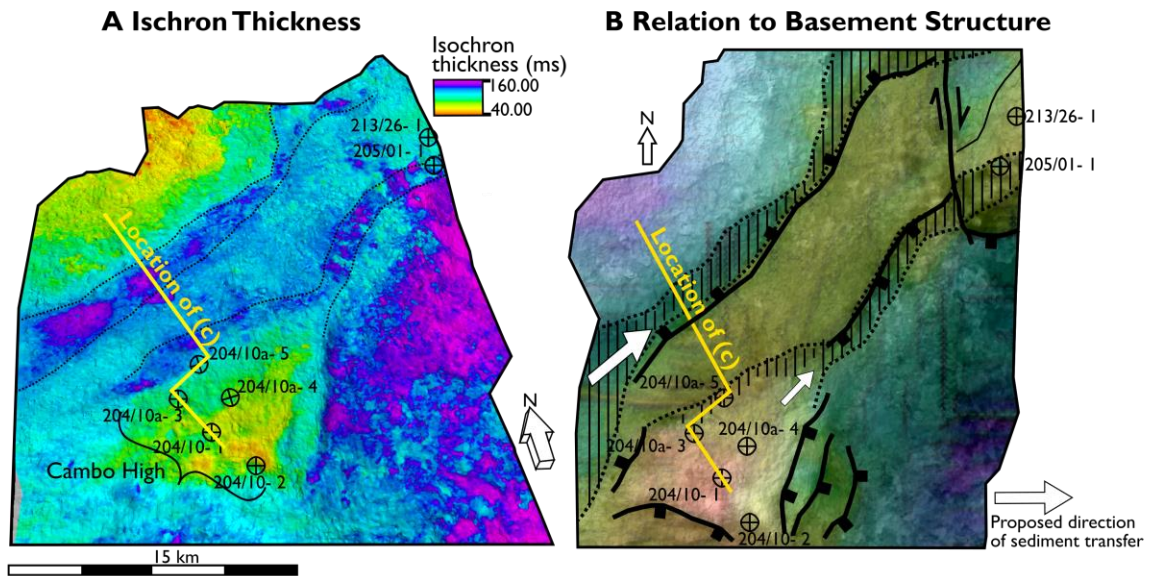
922 Upper Volcaniclastics package through 5 of the Rosebank Wells, SW to NE along the

923 Corona Ridge. Both units are described in detail within the text.



924

925 **Fig 15.** Sequence T45 Enni equivalent lava flows. **A** Seismic line across Enni equivalent lava  
 926 flows. Location shown in Fig 2. **B** RGB Spectral decomposition of Top Basalt horizon. **C**  
 927 Spectral decomposition of Top Rosebank Volcaniclastics horizon, underlying the Top Basalt  
 928 horizon. Ghosting of the overlying lava flow is highlighted in red. **D** Frequency spectrum of  
 929 horizons **B** and **C**. Note the loss in power of the frequency spectrum below the Top basalt  
 930 horizon due to attenuation and scattering of seismic waves in the volcanics.



931

932

933

934

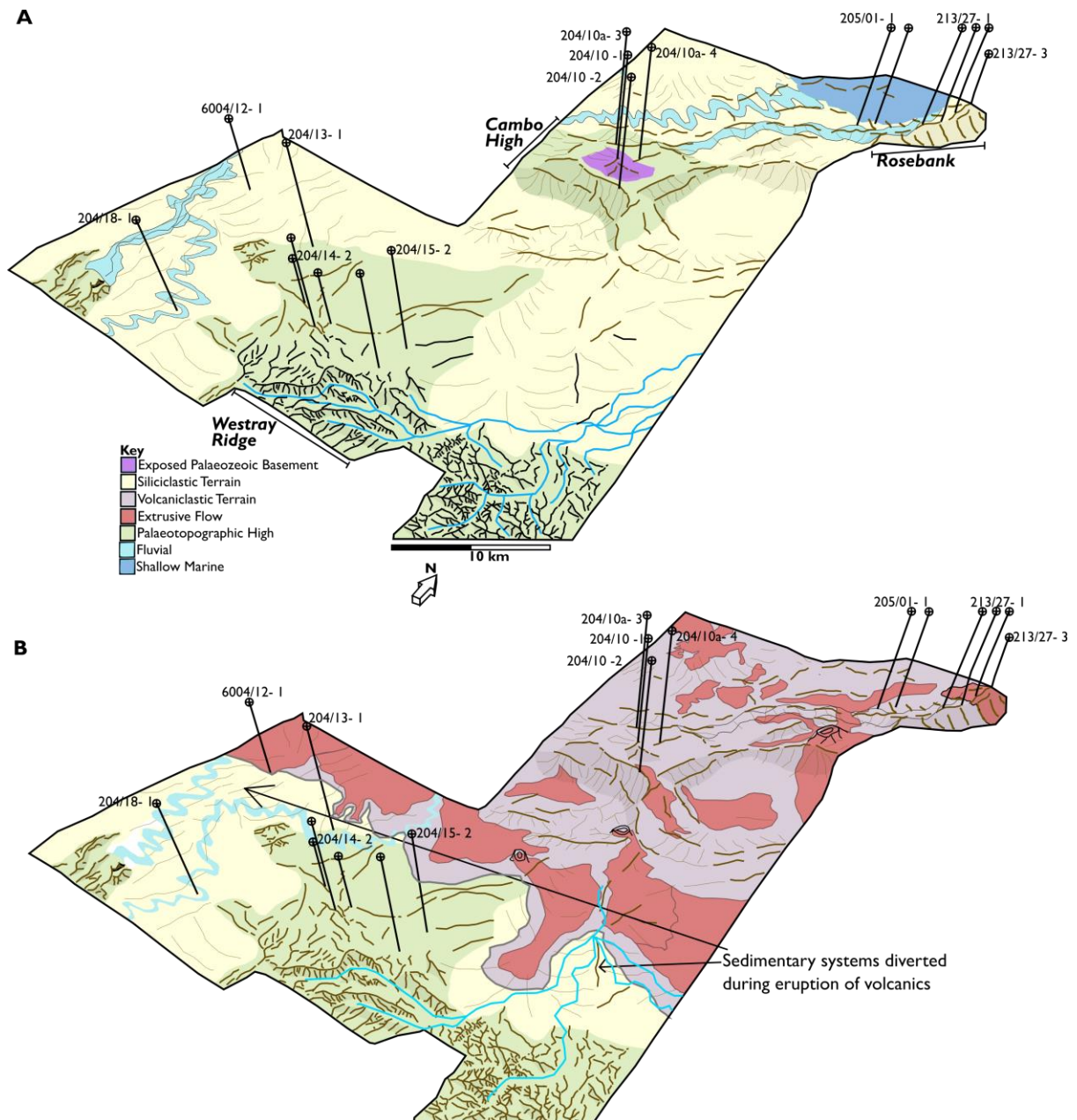
935

936

937

**Fig 16. A** Isochron thickness of the succession between base Colsay I and top Rosebank Volcanics. **B** Isochron thickness displayed as a transparent black-white surface overlain on top of a TWT map of the base Cretaceous. This highlights that the two zones of thickening occur either side of the Corona Ridge. **C** Seismic line taken from the Cambo High and towards the north, demonstrating pronounced thickening of the Colsay sequences just north of 204/10a- 5 Cambo well.





938

939 **Fig 17.** Palaeogeographic reconstructions of the Upper Palaeocene and Lower Eocene of the

940 FSB2011/12 MultiClient GeoStreamer® survey. **A** Entirely siliciclastic palaeoenvironment

941 indicative of Colsay I age sediments. **B** Entirely volcanic palaeoenvironment indicative of the

942 Rosebank Upper Volcaniclastics.